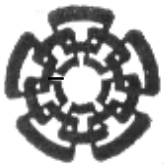

Centro de Investigación y de Estudios Avanzados del Instituto Politécnico Nacional

DEPARTAMENTO DE FÍSICA

Modelos de Interacción Energía Oscura-Materia Oscura en Cosmología

Tesis que presenta

Luis Enrique Galván Torres

para obtener el Grado de

Maestro en Ciencias

en la Especialidad de

Física

Director de tesis: **Dr. Josué De Santiago Sanabria**

Ciudad de México Mayo, 2021

CENTRO DE INVESTIGACION Y DE ESTUDIOS AVANZADOS DEL INSTITUTO POLITECNICO NACIONAL

PHYSICS DEPARTMENT

"Dark Energy-Dark Matter Interacting Models in Cosmology"

Thesis submitted by

Luis Enrique Galván Torres

In order to obtain the

Master of Science

degree, speciality in

Physics

Supervisor: **Dr. Josué de Santiago Sanabria**

Mexico City May, 2021.

Abstract

In this work we studied models of interaction between Dark Energy and Dark Matter at a macroscopic level by modifying the continuity equation of each component. The particular form of the interaction is initially free, but we studied three particular forms. We computed the evolution equations at background level and at first order in perturbations theory. Then, we implemented these equations in the CLASS code. We also added the new feature of choosing the particular interacting model at runtime. Implementing new interacting functions is now straightforward. We obtained the numerical solutions for background quantities and the CMB and Matter Power Spectra. We compared the Background data with available analytical solutions. Finally, we compared all the numerical results with respect to the ΛCDM model ones. These interacting models might reduce the tension in the measurement of the Hubble parameter and can reproduce more general microscopic models.

Resumen

En este trabajo estudiamos modelos de interacción entre la Energía Oscura y la Materia Oscura a un nivel macroscópico, modificando las ecuaciones de continuidad para cada componente. La forma particular de la interacción es inicialmente libre, nosotros estudiamos tres casos particulares. Calculamos las ecuaciones de evolución para el Background y a primer orden en teoría de perturbaciones. Posteriormente, implementamos estas ecuaciones en el código de CLASS. También añadimos la nueva característica de poder elegir el modelo de interacción al momento de correr el código. Implementar nuevos modelos de interacción es ahora sencillo. Obtuvimos las soluciones numéricas para el Background y los Espectros de Materia y del CMB. Comparamos los datos del Background con soluciones analíticas disponibles. Finalmente, comparamos todos los resultados numéricos con los respectivos al modelo cosmológico estándar ΛCDM. Estos modelos de interacción podrían reducir la actual tensión en las mediciones del parámetro de Hubble y pueden reproducir modelos microscópicos más generales.

Acknowledgements

I would like to express the deepest appreciation to all people and situations that brought me to this terminal point in my personal career, particularly in this Master's degree period.

To my thesis advisor Jousé de Santiago who always had the disposition of helping me in any situation and showed me how to be a kind, human and fact-based scientist.

To the National Polytechnic Institute of Mexico (IPN) for give me the opportunity to develop all my human capacities. To my beloved Superior School of Physics and Mathematics (ESFM-IPN), that in addition to knowledge gave me friends and a place where I felt secure, surrounded and guided by dedicated professors to the generation of future scientist.

To the Physics Department of CINVESTAV U. Zacatenco and all the Physics researchers that besides to carry out an international-quality investigation, had the time to share their knowledge in the Master's courses I took and for receiving me as a part of their community.

To CONACYT for gave the financial support for this work, corresponding to the scholarship's call named **"Becas Nacional (Tradicional) 2018 - 2"**, with **CVU-932093**.

Last but not least, to my family who always stayed with me providing their love and support in every step of my life.

Contents

List of Figures

LIST OF FIGURES

List of Tables

LIST OF TABLES

1

Introduction

The modern study of Universe started last century since the development of General Relativity. Images taken of the Universe at different wavelengths and scales suggested that as we go to larger scales the Universe begins to look smooth, equivalent at all points and at all directions. These ideas are now stated as the Cosmological Principles. Following these principles of homogeneity and isotropy the scientists found several solutions to Einstein's equations. One of those solutions was the Friedmann-Robertson-Walker metric that is compatible with the cosmological principles and also allows for a non-static evolution of the Universe. This is important because Hubble found at the beginning of last century experimental evidence for a Universe in expansion and since then many measurements have been made. So, we needed a theory that explains this feature. Various theoretical models of the Universe have been presented, where it is a standard proposal to model the diverse components of the Universe as perfect fluids in a first approach. But the more particular components we add the more difficult it becomes to solve the obtained coupled differential equations. This is why computational tools are extremely important nowadays.

Observations favored a particular model that currently receives the name of ΛCDM model where the Universe is composed by baryons, photons, Dark Energy, Dark Matter and neutrinos. Baryons are essentially the ordinary matter that planets, stars and ourselves are made of. Photons are conceived as relativistic particles that are ruled by the special theory of relativity. Dark Matter is necessary to explain many observed characteristics of the Universe, among them we find the structure formation of the Universe, the galaxy rotation curves, the velocity dispersion in bounded star systems

and the mass of galaxy clusters. All these effects can be explained easily by postulating a component of non-luminous matter, that is the reason this kind of matter is called dark, since it is thought that it do not interact with electromagnetic fields; so it do not absorb, reflect or emit electromagnetic radiation. On the other side Dark Energy is necessary to the expansion of the Universe indicated by supernovae measurements which found it to be accelerated. Another clue for the existence of Dark Energy came from CMB (Cosmic Microwave Background) measurements, they suggest a Universe with spatial curvature close to zero and to achieve this a particular energy density is needed, which is not reached if we only account for baryonic and Dark Matter. The simplest model that takes into account the Dark Energy with these characteristics is the cosmological constant (Λ) model that is a natural degree of freedom in general relativity, where the space-time itself has an intrinsic energy that is not diluted by the expansion, scientists think it could be thought as a zero-point of energy, i.e., a vacuum energy. Another possibility is that the accelerated expansion is carried out by the potential energy of a dynamical field, where the principal difference is that it can be seen as cosmological constant that varies on time and space. Despite the evidence for the existence of Dark Matter and Dark Energy in the Universe, evidence is still indirect and we do not know exactly what they are. This opens a theoretical and experimental opportunity that give us freedom to postulate new ideas to explain some remained issues, for example the actual tension in the measurement of the Hubble parameter, see [2–8]. In this work we proposed that general relativity is the correct theory that describes the Universe at large scales. In that context we proposed an exchange of energy between Dark Matter and Dark Energy via their continuity equations. Dark Energy in this work is the standard one, but we add the characteristic of interact with Dark Matter, so this is an interacting Dark Energy model. Then, this proposal is made at macroscopic level but allowed us to obtain the corresponding CMB and matter Power Spectrum in this interacting scenario. The objective is to study both spectra and analyze the changes that take place in them and in a future work see if it could relax the tension between the measurements of the Hubble constant. These power spectra are highly important because they encode a wide range of cosmological phenomena, and are comparable with experimental results. Therefore, the hypothesis made here can be directly tested.

Based in this model we obtained the cosmological equations in the background and at lineal perturbations level, with their corresponding initial conditions in order to obtain a numerical solution for them. Then we proceeded to implement those equations in the CLASS code [9], we also added the feature of easily adding new interaction models. We used three different models for the interacting scenario, we proposed a simple case where the interaction is carried out by a constant function and two models found in literature [10, 11]. Then we successfully ran the code, and obtained the numerical evolution for all density components at the background level and the matter and CMB Power Spectrum for each of the proposed models. After that, we performed a comparison between the obtained numerical solution and available analytical solutions in order to check if the numerical integration was correct. Once we verified that the solutions agreed with the analytical ones we analyzed the results and made the pertinent conclusions.

In literature there are many alternative models to ΛCDM, even there are proposed modified versions of general relativity. Here we present one of this possibilities that need to be verified or excluded. It presents a macroscopic view without the necessity to specify the underlined microscopic nature of the phenomena. This model also can account for several different microscopic models and have the feature of be flexible, since we can add diverse interacting models in an easy way. And moreover, we can obtain the CMB and matter Power Spectra with a simple running of CLASS. In a future work this proposal can be tested and the parameters fitted with the available experimental data, technically the implementation in CLASS is harder to code than making the fitting, for example with aid of Montepython [12].

2

Theory

2.1 Cosmology foundations

2.1.1 The Cosmological Principle

Modern cosmology is based on the simple but powerful assumption that on large scales the Universe is homogeneous and isotropic, as supported by observations [1]. Homogeneity means that all physical conditions are the same at every point of the Universe and isotropy refers to the fact that this physical conditions do not depend on the direction of observation. This implies that there are no special places in the Universe and this statement has validity only at scales of Mpc (1pc $\approx 3.08 \times 10^{16}$m) where the Universe looks smooth.

2.1.2 The Doppler Effect

In 1842, Johann Christian Doppler asserted that if an observer receives an emitted wave by a source in relative motion, the wavelength measured will be shifted proportionally to the velocity of the source projected along the line of sight

$$\frac{\Delta\lambda}{\lambda} = \frac{\mathbf{v}\cdot\mathbf{n}}{c}, \tag{2.1}$$

with c the celerity of the wave and $\mathbf{n}$ the unit vector along the line of observation. It was suggested and then proved that this relation holds for sound and electromagnetic waves [13].

It is useful to define the redshift parameter as

$$z \equiv \frac{\Delta\lambda}{\lambda}, \tag{2.2}$$

when z is positive the wave is said to be red-shifted and if it is negative blue-shifted.

2.1.3 The Hubble Law

Another last century experimental result is that objects in the Universe are moving away from us, because emitted light from distant objects is received by us redshifted due to the Doppler effect. Moreover it was found by Edwing Hubble [14], that the recession velocity $\mathbf{v}$ of a galaxy is proportional to its position $\mathbf{r}$

$$\mathbf{v} = H_0\mathbf{r}, \tag{2.3}$$

where H_0 is the constant of proportionality known as the Hubble constant. This relation states that velocities of objects increase with the distance they are, so we can infer that at cosmological scales objects are moving away from us. Note that this law breaks at small scales because if we observe nearby objects we will see they have peculiar velocities not proportional to their distance. This particular relation between velocity and distance also implies that all observers see the same effect no matter the place of observation, i. e., it is left unchanged by a change of origin and therefore is compatible with the Cosmological Principle.

2.2 Homogeneous and isotropic Universe

2.2.1 Units convention and notation

From now on we will adopt the unit convention $c = \hbar = k_b = 1$ in most of the expressions. Einstein's summation convention is used throughout all the following work and as usual Greek alphabet run for space-time index coordinates $\{t, x, y, z\}$ and Latin alphabet run only for spatial coordinates $\{x, y, z\}$.

2.2.2 Coordinate choice in a homogeneous and isotropic Universe

The fact that the Universe is homogeneous and isotropic implies that for a given time all spatial points and directions are equivalent, in that sense physical quantities depend on time but not on the spatial coordinates. We then can construct a coordinate system that preserves this characteristic in the following way; we start from an initial homogeneous spatial hypersurface and we assign it the time t_1 and some arbitrary spatial coordinates,

we put observers in each point and define a new hypersurface as the collection of all points such that observer's clocks measure t_2. We assign to this hypersurface the time coordinate t_2, and some spatial coordinates such that each of our observers keeps fixed spatial coordinates. We can repeat this process, until all time-spatial points map to a coordinate system with fixed spatial coordinates and a common proper time. This particular coordinate system is called Comoving Coordinate System and will be denoted by

$$\{t, x, y, z\}. \tag{2.4}$$

Note that a particular transformation $t \to t'(t)$ or $x_i \to x_i'(x_i)$ does not modify the homogeneity of equal-time hypersurfaces. But in a more general transformation $t \to t'(t, x_i)$ equal-time hypersurfaces homogeneity no longer holds. That is the reason we can use spherical coordinates as a comoving coordinate system

$$\{t, r, \theta, \phi\}. \tag{2.5}$$

2.2.3 The FRW metric

Standard cosmology is based in the fact that general relativity is the correct theory of gravity on cosmological scales. So, if we impose the conditions of homogeneity and isotropy by pure geometrical arguments we can find the metric that describes this situation. This metric is known as Friedmann-Robertson-Walker (FRW) metric, see [15–18].

$$ds^2 = -dt^2 + a(t)^2\left(\frac{dr^2}{1-kr^2} + r^2 d\theta^2 + r^2 sin^2(\theta) d\phi^2\right), \tag{2.6}$$

where $a(t)$ is known as the expansion parameter and takes into account the time evolution of the Universe, the constant parameter k is the three dimensional space curvature. Note that k can be positive, negative or zero (plane space) and that we have used the convention $c = 1$ for the speed of light c.

It is common to define a conformal time η by the expression

$$dt = a d\eta, \tag{2.7}$$

in order to have the expansion factor as an overall factor in the metric

$$ds^2 = a(\eta)^2\left(-d\eta^2 + \frac{dr^2}{1-kr^2} + r^2 d\theta^2 + r^2 sin^2(\theta) d\phi^2\right). \tag{2.8}$$

2.2.4 Distances in cosmology

There are different ways to specify the distance between two points in cosmology. The reason is that in an expanding Universe the distance between comoving objects are constantly changing and that observers, for example in Earth's comoving system when observing a star, we are looking to radiation emitted some time ago in the past. In order to solve this issues let us introduce some useful parameters. Because of the expansion, light received in Earth is redshifted, where redshift is defined as the fractional Doppler shift of its emitted light resulting from radial motion

$$z \equiv \frac{\nu_e}{\nu_o} - 1 = \frac{\lambda_o}{\lambda_e} - 1, \tag{2.9}$$

where ν and λ are frequency and wavelength of light and subscripts e, o denote emitted and observed light. As wavelength is proportional to the time between crests we have

$$\frac{\lambda_o}{\lambda_e} = \frac{a(t_o)}{a(t_e)}, \tag{2.10}$$

with t_o, t_e the time of observation and emission of light. Now we can obtain the relation between redshift and the expansion parameter

$$1 + z = \frac{a(t_o)}{a(t_e)}, \tag{2.11}$$

where is common to set the time of observation to be the actual time.

Relation 2.11 is important because redshift is and easy to measure parameter, and usual astronomical experiments are reported with this parameter. So in order to compare our models with experimental data, all distances are reported in terms of redshift.

Other parameters needed in order to define distances in cosmology are the Hubble parameter H_0 defined in Eq.(2.3). It is usually written $H_0 \equiv 100h\text{kms}^{-1}\text{Mpc}^{-1}$, where h is a dimensionless number parameterizing the existing uncertainty in the value of H_0, it is often said that $(0.6 < h < 0.9)$. If light velocity is set to one, then the distance traveled by light in the Hubble time (defined as the inverse of H_0), is known as the Hubble distance

$$d_H \equiv \frac{1}{H_0} = 3000h^{-1}\text{Mpc} \tag{2.12}$$

2.2.5 The comoving distance

Consider light traveling in radial and null trajectories

$$ds^2 = 0 = -ad\eta + adr, \tag{2.13}$$

we can obtain the radial comoving distance r by integrating and applying the chain rule to change the integration variable from the conformal time η to the redshift parameter z, along with the definitions of the Hubble parameter and Friedmann equation to obtain

$$r(z) = d_H \int_0^z \frac{dz'}{E(z')}, \tag{2.14}$$

with $E(z) \equiv \sqrt{\Omega_r(1+z)^4 + \Omega_m(1+z)^3 + \Omega_\Lambda}$. And Ω_i the density parameter for each component of the spatially flat Universe.

2.2.6 Luminosity distance

We can not measure directly the comoving distance, but we can measure for example a star's energy density flux f received by an astronomical observatory and if we know the luminosity of and object L, assuming valid the inverse square law for L we obtain

$$4\pi d_{lum}^2 = \frac{L}{f}. \tag{2.15}$$

Notice that d_{lum} is not the real distance to the object because the Universe is expanding and therefore the inverse square law does not hold. In that sense d_{lum} is only a parameter for distance since it is a growing function of the real distance. If we were in a static space, the energy flux received would be $f = \frac{L}{4\pi r^2}$. But according to [1], due to the expansion the photons lose energy $\propto (1+z)$ and arrive less frequently $\propto (1+z)$. So the received energy flux is

$$f = \frac{L}{4\pi r^2 (1+z)^2}, \tag{2.16}$$

so we can infer

$$d_{lum} = r(1+z), \tag{2.17}$$

with r the comoving distance defined in the previous section.

2.2.7 Angular diameter distance

If we now consider and object of physical length ℓ lying perpendicular to our line of sight, the angular diameter distance is a measure of how long the object appears to be under the assumption of flat space

$$d_{ang} \equiv \frac{\ell}{2sin(\frac{\theta}{2})} \approx \frac{\ell}{\theta} \quad for \quad \theta \ll 1. \tag{2.18}$$

Now in a spherical coordinate system with origin at where we are measuring and if the object is at comoving radial coordinate r, we would have

$$ds = \ell = a(t_e) r d\theta, \tag{2.19}$$

where we have used the metric at the emission time. Taking into account Eq.(2.11) for the expansion of the Universe we obtain

$$d\theta = \frac{\ell}{a(t_e)r} = \frac{\ell(1+z)}{r}, \tag{2.20}$$

from where we obtain the useful relation between d_{ang} and the comoving distance r

$$d_{ang} = \frac{r}{1+z}. \tag{2.21}$$

2.2.8 The Friedmann equations

If we consider a universe filled with a perfect fluid with four-velocity u^μ, we then have the stress-energy tensor

$$T^{\mu\nu} = (\rho + p)u^\mu u^\nu + p g^{\mu\nu}, \tag{2.22}$$

with ρ and p the proper energy density and pressure of fluid in the fluid rest frame which is defined by condition $u^i = 0$ (i stands for spatial components).

Now we can compute the Einstein's equations

$$G^\alpha_\beta \equiv R^\alpha_\beta - \frac{1}{2}\delta^\alpha_\beta R - \delta^\alpha_\beta \Lambda = 8\pi G T^\alpha_\beta, \tag{2.23}$$

here

$$R^\alpha_\beta \equiv g^{\alpha\gamma}\Big(\partial_\delta \Gamma^\delta_{\gamma\beta} - \partial_\beta \Gamma^\delta_{\gamma\delta} + \Gamma^\delta_{\gamma\beta}\Gamma^\sigma_{\delta\sigma} - \Gamma^\sigma_{\gamma\delta}\Gamma^\delta_{\beta\sigma}\Big), \tag{2.24}$$

is the Ricci tensor defined in terms of Christoffel symbols

$$\Gamma^\alpha_{\mu\nu} = \frac{1}{2} g^{\alpha\beta}(\partial_\mu g_{\beta\nu} + \partial_\nu g_{\beta\mu} - \partial_\beta g_{\mu\nu}). \tag{2.25}$$

R is the Ricci curvature scalar $R \equiv R^{\alpha}_{\alpha}$ and G, Λ are the gravitational and cosmological constants respectively.

Solving, we obtain two independent equations known as Friedmann Equations

$$\frac{\dot{a}^2 + k}{a^2} = \frac{8\pi G\rho + \Lambda}{3}, \tag{2.26}$$

$$\frac{\ddot{a}}{a} = -\frac{4\pi G}{3}\Big(\rho + 3p\Big) + \frac{\Lambda}{3}, \tag{2.27}$$

where dot represents a derivative respect to cosmological time t.

We can combine the above equations and obtain a non-independent third equation

$$\dot{\rho} = -3H(\rho + p), \tag{2.28}$$

where the Hubble parameter

$$H \equiv \frac{\dot{a}}{a}, \tag{2.29}$$

is defined.

2.2.9 Universe filled with mixture of non-interacting fluids

In this case Eq.(2.28) holds separately for each component and implementing a particular equation of state $p = p(\rho)$ we can substitute $\dot{\rho}$ in Eq.(2.26) to obtain

$$H^2 = \frac{8\pi G}{3}\sum_i \rho_i, \tag{2.30}$$

where the index i stands for each component in the Universe. Note that with simple redefinitions we can include as Universe components the curvature k and the cosmological constant Λ. Explicitly we have

$$\rho_k \equiv -\frac{3k}{8\pi G a^2}, \tag{2.31}$$

$$\rho_\Lambda \equiv \frac{\Lambda}{8\pi G}. \tag{2.32}$$

2.2.10 Universe components in the Standard Cosmological Model

The standard cosmological model, named ΛCDM model, lays on the assumption of the cosmological principle in an expanding Universe and takes General Relativity as the correct theory of gravity on cosmological scales. With respect to the contents of the Universe this model considers

- **Dark Energy**. Associated to the cosmological constant Λ and currently associated with a vacuum energy. It is believed to be responsible of actual expansion of the Universe against attractive gravitational forces and has negative pressure $p_\Lambda = -\rho_\Lambda$.
- **Cold Dark Matter (CDM)**. It is a component postulated in order to explain the large scale structures' gravitational effects that can not be explained with the current observed quantity of normal matter. For example the galaxy rotation curves or gravitational lensing of light by galaxy clusters. It is believed to be non-baryonic, dissipationless (can not cool by radiating photons), collisionless and cold (its velocity is much less than the speed of light). This implies an equation of state $p(\rho) = 0$.
- **Baryonic Matter**. It includes normal matter from which stars, planets and galaxies are made.
- **Radiation**. It is mostly important at the beginning of the Universe and it is responsible of the observed Cosmic Microwave Background (CMB).

2.2.11 Brief history of the Universe according to Standard Cosmological Model

As we trace back in time we find the Universe in a singular state. Colloquially people says that there was a Big Bang, but formally it refers to the fact that space-time itself originated from a singularity according to a Penrose's theorem [19]. Then the model postulates an epoch known as cosmic inflation where the Universe expands exponentially and solves some issues of the theory [20]. After that Friedmann equations rule the Universe evolution.

A pedagogical way to study the evolution of the Universe is to take the Friedmann equations and set as an approximation $k = \Lambda = 0$ and no contribution from Dark

Matter, even if they are not zero now, they would be negligible in early stages of the Universe. In that situation and assuming instantaneous transition between radiation domination and matter domination we can solve and describe the evolution of the Universe in terms of time or temperature. A good description is given in [1] where we found Table (2.1)

Time	Temperature	What is going on?
$t < 10^{-10}$s	$T > 10^{15}$K	Open to speculation.
10^{-10}s < t < 10^{-4}s	10^{15}K > T > 10^{12}K	Free electrons, quarks, photons, neutrinos; everything is strongly interacting with everything else.
10^{-4}s < t < 1s	10^{12}K > T > 10^{10}K	Free electrons, protons, neutrons, photons, neutrinos; everything is strongly interacting with everything else.
1s < t < 10^{12}s	10^{10}K > T > 10^{3}K	Protons and neutrons have joined to form atomic nuclei, and so we have free electrons, atomic nuclei, photons, neutrinos; everything is strongly interacting with everything else except the neutrinos, whose interactions are now too weak. The Universe is still radiation dominated.
10^{12}s < t < 10^{13}s	10^{3}K > T > 3000K	As before, except that now the Universe is matter dominated.
10^{13}s < t_0	3000K > T > 3K	Atoms have now formed from the nuclei and the electrons. The photons are no longer interacting with them, and are cooling to form what we will see as the microwave background.

Table 2.1: Brief history of the Universe from [1]

2.2.12 Decoupling and the origin of Cosmic Microwave Background

The Cosmic Microwave Background (CMB) is radiation that bathes the Earth from all directions, Penzias & Wilson discovered it in 1965 [21]. This radiation has an energy distribution analogue to a black-body with temperature $T_0 = 2.725 \pm 0.001$K. The origin of this radiation dates back to when the Universe was smaller and hotter so photons were able to highly interact with electrons preventing the formation of atoms. The Universe was a sea of free nuclei, electrons and photons interacting principally via scattering. As the Universe expanded and cooled mean energy of photons decreased, so progressively atoms could form and photons were free to travel from that time until the present days. This process in known as decoupling.

All photons we observe as CMB radiation have traveled a large distance comparable to the size of the observable Universe, they all come from a spherical surface called the last scattering surface, with a very large radius and center in the point of observation. At decoupling, when this photons set free their energies were not in the microwave spectrum but as they traveled and the Universe expanded, we finally observe them in the microwave spectrum.

2.2.13 Overview of Standard Cosmology

This model is called standard because it is the simplest model that explains most features of the observable Universe, among them we find:

- The accelerating expansion of the Universe.
- The origin and structure of the cosmic microwave background.
- The large scale distribution of galaxies.
- The observed abundances of light elements.

But some issues still remain, for example:

- The cosmological constant problem. Which refers to the disagreement between the observed values of vacuum energy density and the theoretical large value of zero-point energy suggested by quantum field theory.
- The Dark Energy presents no dynamics as ρ_Λ is constant.

- An homogeneous and isotropic Universe expanding preserves this characteristics through its evolution and do not explain the structure formation at local scales.

2.3 Linear Perturbations Theory

Evidence suggests we live in a nearly spatially flat Universe [22], so it is common to set $k = 0$ as a good approximation to reality. Also, if we want to explain structure formation in the Universe at lower scales where homogeneity and isotropy no longer hold we will have to allow for small perturbations in the metric and the stress-energy tensor.

$$g_{\mu\nu}(t, \mathbf{x}) = \overline{g}_{\mu\nu}(t) + \delta g_{\mu\nu}(t, \mathbf{x}), \tag{2.33}$$

$$T_{\mu\nu}(t, \mathbf{x}) = \overline{T}_{\mu\nu}(t) + \delta T_{\mu\nu}(t, \mathbf{x}), \tag{2.34}$$

where $\overline{g}_{\mu\nu}(t)$ and $\overline{T}_{\mu\nu}(t)$ stand for metric and stress-energy tensor spatial averages in a linearly perturbed Universe. Note that linear perturbations $\delta g_{\mu\nu}(t, \mathbf{x})$ and $\delta T_{\mu\nu}(t, \mathbf{x})$ depend both on space and time and that they must be symmetric tensors, since $g_{\mu\nu}(t, \mathbf{x})$ and $T_{\mu\nu}(t, \mathbf{x})$ are symmetric. Therefore each one contains ten degrees of freedom. In 1980, Bardeen [23] showed that these perturbations decompose in the basis of scalar, vector, and tensor perturbations under spatial rotations.

2.3.1 Metric perturbations

In general we can decompose metric perturbations in

$$\delta g_{00} = -2a^2\phi, \tag{2.35}$$

$$\delta g_{0i} = a^2 B_i, \tag{2.36}$$

$$\delta g_{ij} = 2a^2 C_{ij}. \tag{2.37}$$

The $\{0i\}$ and $\{ij\}$ perturbation components can be further decomposed into scalar, vectors and tensor contributions

$$B_i = B_{,i} - S_i \tag{2.38}$$

$$C_{ij} = -\Psi\delta_{ij} + E_{,ij} + F_{(i,j)} + \frac{1}{2}h_{ij}, \tag{2.39}$$

with ϕ, B, Ψ, E scalar perturbations, F_i, S_i vector perturbations and h_{ij} tensor perturbation. These perturbations are restricted, vector perturbations are divergence-free, so from the original six vectorial degrees of freedom (three for each one) only remain four. And tensor perturbation which is symmetric, divergence-free ($h^j_{ij,} = 0$) and trace-free ($h^i_i = 0$) stands for two degrees of freedom.

In the vacuum, scalar and vector perturbations vanish and tensor perturbations account for gravitational waves [24]. In the presence of matter, scalars can be seen as a response of the metric to the presence of irrotational matter, vectors represent the response of metric to vorticity and has no analogue with Newton's theory of gravity. It is common to consider that vorticity of the different species of the Universe decays with time, so vector perturbations are neglected and tensor plays only a small role in CMB anisotropies, so we will focus on linear scalar perturbations of the metric

$$\{\phi, B, \Psi, E\} \tag{2.40}$$

The general metric in linear perturbations theory is described by the line element,

$$ds^2 = -(1+2\epsilon\phi)d\eta^2 + 2a\epsilon\partial_i B d\eta dx^i + a^2\left[(1-2\epsilon\psi)\delta_{ij} + 2\epsilon\partial_i\partial j E\right]dx^i dx^j, \tag{2.41}$$

with η conformal time, a=a(η) the expansion factor and ϕ, ψ, E, B functions of space and time assumed to be proportional to $\epsilon \ll 1$ in accordance with perturbation theory.

2.4 Gauges and time slicing

A gauge is a coordinate transformation $x_\mu \to x_\mu + \epsilon_\mu$ that preserves the linearity of perturbations, this restricts ϵ_μ to be very small in every point.

Note that for example in energy density perturbations

$$\delta\rho(\eta, x^i) \equiv \rho(\eta, x^i) - \overline{\rho}(\eta), \tag{2.42}$$

$\rho(\eta, x^i)$ is a local and well defined quantity, while $\overline{\rho}(\eta)$ is a spatial average that depends on the choice of equal-time hypersurfaces going through the point (η, x^i). In that sense $\delta\rho(\eta, x^i)$ is said to be gauge dependent, because a particular gauge defines a particular kind of equal-time hypersurfaces or time slicing.

In an idealized FRW Universe there is only one time slicing compatible with the Cosmological Principle, but in linear perturbations theory there are various choices of time slicing compatible with perturbations theory, i.e., we can find multiple equal-time hypersurfaces such that all physical quantities remains close to their average value.

This freedom of choosing between different gauges without changing physical results has the effect that some solutions in perturbations theory are gauge modes with no physical meaning. So we have two options

- Work with non-trivial combinations of stress-energy tensor and metric components with the property of being gauge invariant and obtain and solve equations of motion where gauge degrees of freedom no longer account.

- Fix a particular gauge, with the possible disadvantage that some results will have a particular form depending on the gauge choice. Note that choosing a particular gauge implies to set fixed two degrees of freedom. Since in general we have to specify the ϵ_μ component of the gauge transformation which accounts for ϵ_0 and the potential e such that $\epsilon_i = \partial_i e$.

It is important to stress that in practice physical results do not depend on which of the two above ways we took since physical quantities are gauge independent.

In the following sections we will fix a particular gauge.

2.4.1 Newtonian Gauge

In the Newtonian gauge the non-diagonal scalar perturbations of the metric are imposed to vanish

$$E = B = 0. \tag{2.43}$$

The result is that since metric perturbation elements are diagonal, calculations under this gauge become easy to handle. Another characteristic of this gauge is that Ψ and ϕ have direct physical interpretation; Ψ for lower scales reduces to the classical gravitational potential and ϕ can be thought as a local deviation of the expansion parameter a.

2.4.2 Synchronous Gauge

In the synchronous gauge, introduced by Lifshitz [25] in 1946, the components g_{00} and g_{0i} of the metric tensor are by definition unperturbed

$$\phi = B = 0. \tag{2.44}$$

It is not difficult to show by computing the geodesic equation that in this gauge $u_i = 0$ is a solution of the geodesic equation (since the Christoffel symbols Γ^i_{00} vanish). This means that there exists a set of comoving observers who fall freely without changing their spatial coordinates, they are called fundamental comoving observers. This gauge is not free of issues [26], for example, when the trajectory of two fundamental comoving obervers intersect the coordinates become singular (one spacetime point would have two different labels); or the conditions (2.44) do not remove completely the gauge modes since the choice of initial time and initial spatial coordinates for fundamental comoving obervers is arbitrary. This situation led Bardeen in 1980 [23] to formulate alternatives dealing with gauge invariant quantities.

In this work we will work mostly in the Synchronous gauge, the reason is that we are not treating with direct spacetime properties and that it allows us to obtain simple expressions for the equations of motion and only a single equation for the evolution of linear perturbations (see Eq.(2.100)).

2.5 Calculations in Synchronous Gauge

The principal aim of this section is to derive the equations of evolution for background quantities and linear scalar perturbations in the synchronous gauge for the Dark Energy-Dark Matter interacting model.

2.5.1 Linear Scalar Perturbations for spatially plane FRW metric

Matrix elements of metric 2.41 in synchronous gauge and expanded at first order in ϵ are

$$g_{00} = -a^2 + O\left(\epsilon^2\right), \tag{2.45}$$

$$g_{0i} = O\left(\epsilon^2\right), \tag{2.46}$$

$$g_{ii} = a^2 - 2a^2\epsilon(\Psi - E_{,ii}) + O\left(\epsilon^2\right), \tag{2.47}$$

$$g_{ij} = 2a^2\epsilon E_{,ij} + O\left(\epsilon^2\right) \quad for \quad i \neq j, \tag{2.48}$$

where as usual we have used the correspondence $\{\eta, x, y, z\} \rightarrow \{0, 1, 2, 3\}$ with $i, j = \{1, 2, 3\}$ and comma indicates partial derivation.

2.5.2 Stress-energy tensor perturbations

Similarly we need to specify four scalar degrees of freedom for the stress-energy tensor.

- $\delta\rho(\eta, x^i)$ the energy density perturbation.
- $\delta p(\eta, x^i)$ the pressure perturbation.
- The potential v of the irrotational component of the flux of energy $\delta T^0_i = \partial_i v$
- The potential s of the shear stress or anisotropic stress $\delta T_{ij} = (\partial_i\partial_j - \frac{1}{3}\delta_{ij})s$.

2.5.2.1 Stress-energy tensor perturbations of a perfect fluid

If we consider that matter can be modeled with a perfect fluid, where microscopic interactions impose local thermodynamical equilibrium, the pressure is then isotropic and therefore we have the condition for the shear stress s

$$s = 0 \tag{2.49}$$

Moreover for a perfect fluid pressure perturbations obey $\delta p = c_a^2\delta\rho$, with c_a the adiabatic sound speed inferred from the equation of state of the fluid. So, we can describe a perfect fluid in a linearly perturbed Universe with the reduced set

$$\{\delta\rho(\eta, x^i), v\} \tag{2.50}$$

Notice that normalization $u^\mu u_\mu = -1$ along with perturbed metric and the perfect fluid stress-energy tensor implies at first order in perturbations

$$u_\mu = a[-1, \partial_i v], \qquad u^\mu = \frac{1}{a}[1, \partial^i v], \tag{2.51}$$

with $v^i = \frac{dx^i}{d\eta}$ a non rotational velocity. Strictly speaking v^i is not the three-velocity because we have now in consideration perturbations in the metric, i.e., adx^i is not a proper distance and $ad\eta$ is not a proper time. If perturbations are small enough then $v^i \ll 1$ and this velocity becomes a good approximation to the three-velocity.

We can now compute the stress-energy tensor for perfect fluid in the perturbed and plane FRW metric through equations (2.22), (2.45), (2.46), (2.47), (2.48), and (2.51). Introducing the fluid equation of state defined by

$$w \equiv \frac{p}{\rho}, \tag{2.52}$$

we obtain at first order in perturbations

$$T^{00} = \frac{\rho}{a^2} + \epsilon\frac{\delta\rho}{a^2} + O\left(\epsilon^2\right), \tag{2.53}$$

$$T^{0i} = \epsilon\frac{(\rho + w\rho)v_{,i}}{a^2} + O\left(\epsilon^2\right), \tag{2.54}$$

$$T^{ii} = \frac{w\rho}{a^2} + \epsilon\frac{w\left(\rho\left(2\Psi - 2E_{,ii}\right) + \delta\rho\right)}{a^2} + O\left(\epsilon^2\right), \tag{2.55}$$

$$T^{ij} = -2\epsilon\frac{w\rho E_{,ij}}{a^2} + O\left(\epsilon^2\right). \tag{2.56}$$

We would like to emphasize that background functions a and ρ only depend on time while perturbations functions $\Psi, E, \delta\rho, v$ depend both on space and time.

2.6 The Interacting Model

2.6.1 Generalized Continuity Equation

We introduce the energy transfer four-vector Q^μ defined by

$$Q^\mu \equiv \nabla_\nu T^{\mu\nu}. \tag{2.57}$$

Following [27] we may decompose Q^μ in components parallel and orthogonal to matter four-velocity described by $T^{\mu\nu}$

$$Q^\mu = Qu^\mu + f^\mu, \tag{2.58}$$

with $f^\nu u_\nu = 0$ by definition.

We propose an interaction between Dark Energy and Dark Matter via their continuity equations

$$\nabla_\nu T^{\mu\nu}_{DM} = Q^\mu_{DM} = -Q^\mu_{DE} = -\nabla_\nu T^{\mu\nu}_{DE}. \tag{2.59}$$

This assumption essentially introduces an energy conversion between Dark Energy and Dark Matter and gives no clue about the micro-physical description of the phenomena but allows us to subject the model to the observations. This useful feature makes that interacting models have been studied for some authors, see for example [27–29].

We are now able to compute the continuity equation using

$$\nabla_\nu T^{\mu\nu} = \partial_\nu T^{\mu\nu} + \Gamma^\mu_{\nu\alpha} T^{\alpha\nu} + \Gamma^\nu_{\nu\alpha} T^{\alpha\mu}. \tag{2.60}$$

Computing Q and f^μ is straightforward with the aid of the metric and the above expressions

$$Q = Q^\mu u_\mu, \tag{2.61}$$

$$f_\nu = (g_{\mu\nu} + u_\mu u_\nu) Q^\mu, \tag{2.62}$$

since we know the projection operator $P_{\mu\nu} \equiv (g_{\mu\nu} + u_\mu u_\nu)$ is orthogonal to four-velocity.

Explicitly, for the perfect fluid model at first order in perturbations we have

$$\begin{aligned} Q = &-\frac{3(w+1)\rho a' + a\rho'}{a^2} - \epsilon \frac{3(w+1)a'\delta\rho}{a^2} \\ &- \epsilon \frac{(\delta\rho)' - (w+1)\rho\left(-\nabla^2 E' - \nabla^2 v + 3\Psi'\right)}{a} + O(\epsilon^2), \end{aligned} \tag{2.63}$$

$$f_i = \frac{\epsilon}{a}\left[wa(\delta\rho)_{,i} + \left((1+w)\rho a' + (1+w)a\rho + wa\rho'\right)v_{,i}\right] + O(\epsilon^2). \tag{2.64}$$

2.6.2 Fluid Equations for Dark Matter and Dark Energy

The Dark Energy in this work is defined to have a stress-energy tensor proportional to the metric

$$T^{\mu\nu}_{DE} \equiv V g^{\mu\nu}, \tag{2.65}$$

and by comparison with a perfect fluid stress-energy tensor, Eq.(2.22), we note that

$$V = \rho_\Lambda = -P_\Lambda. \tag{2.66}$$

For simplicity from now on we will use the subscript Λ to denote Dark Energy as defined by Eq(2.65), but this Dark Energy model is more general than a cosmological constant model and if we had a spatially homogeneous and non time dependent vacuum energy $\nabla_\nu V = 0$, we would recover a Λ model with $\Lambda = 8\pi G V$.

Since in this Dark Energy model there are no particles flow, then the four-velocity of a fluid element. As in regards of Eq.(2.58) we need a four-velocity direction to decompose the energy flow, we choose this to be the Dark Matter four-velocity introduced in Eq.(2.51).

With all this in consideration we can obtain Q and f_i for the particular cases of Dark Matter and Dark Energy by putting the corresponding equation of state for each type of fluid in Eqs.(2.63) and (2.64), namely

$$w_{DE} = -1, \qquad w_{DM} = 0. \tag{2.67}$$

The above values are the standard ones, (see [30, 31]).

So we get the expressions for Dark Matter

$$Q^{DM} = -\left(\frac{3\rho_c a' + a\rho_c'}{a^2}\right) + \epsilon\left(-\frac{3a'\delta\rho_c}{a^2} - \frac{(\delta\rho_c)'}{a} + \frac{\rho_c}{a}(-\nabla^2 E' - \nabla^2 v + 3\Psi')\right) + O(\epsilon^2), \tag{2.68}$$

$$f_i^{DM} = \epsilon\frac{\rho_c}{a}(a' v_{,i} + a v_{,i}') = \epsilon\frac{\rho_c}{a}(a v_{,i})' + O(\epsilon^2). \tag{2.69}$$

The corresponding equations for Dark Energy are

$$Q^{DE} = -\frac{\rho_\Lambda'}{a} - \epsilon\frac{\delta\rho_\Lambda'}{a} + O(\epsilon^2), \tag{2.70}$$

$$f_i^{DE} = -\epsilon(\rho_\Lambda' v_{,i} + \delta\rho_{\Lambda,i}) + O(\epsilon^2). \tag{2.71}$$

Where we have used the standard notation for Dark Matter density ρ_c and Dark Energy density ρ_Λ.

2.6.3 Background Equations

Equating zero order perturbation terms of Eq.(2.59) and implementing Eq.(2.30) we obtain the coupled background equations

$$\rho_\Lambda' = aQ, \tag{2.72}$$

$$\rho_c' = -aQ - 3\rho_c H, \tag{2.73}$$

$$a' = a^2 H. \tag{2.74}$$

It is important to stress that since

$$Q = Q(\rho_\Lambda, \rho_c, a, H), \tag{2.75}$$

no new degrees of freedom are added to the model.

We can also see from the background equations that

- $Q > 0$ implies an energy transference from Dark Matter to Dark Energy since $\rho_\Lambda' \propto Q$.
- $Q < 0$ implies an energy transference from Dark Energy to Dark Matter since $\rho_c' \propto -Q$.
- $Q = 0$ reduces to the Standard Cosmological Model (ΛCDM).

2.6.4 Models for Q

Choosing a particular model of Q from now on called the interacting function, determines the dynamics of the model and closes the equation system in order to solve it. Next we present some models proposed in literature.

2.6.4.1 Constant interacting function

The simplest model we can propose is a constant interacting function

$$Q = Q_0. \tag{2.76}$$

Despite its simplicity it is not analytically solvable.

2.6.4.2 Martinelli's Model

The Martinelli's model proposed in [11] reads

$$Q = -q_0 H \rho_\Lambda, \tag{2.77}$$

with q_0 a dimensionless parameter and H the Hubble parameter.

This model has an analytical solution at the background level, supposing a reduced model where the Universe is filled only with ρ_c and ρ_Λ

$$H^2 = \frac{8\pi G}{3}(\rho_c + \rho_\Lambda). \tag{2.78}$$

In that case we obtain

$$\rho_c = \rho_c^0 a^{-3} + \rho_\Lambda^0 \frac{q_0}{q_0 - 3}\left(a^{-3} - a^{-q_0}\right), \tag{2.79}$$

$$\rho_\Lambda = \rho_\Lambda^0 a^{-q_0}, \tag{2.80}$$

with ρ_c^0, ρ_Λ^0 the densities at the present time.

2.6.4.3 Wang's Model

This model was proposed in [10] and the interaction has the functional form

$$Q = 3\alpha H \frac{\rho_c \rho_\Lambda}{\rho_c + \rho_\Lambda}, \tag{2.81}$$

with α a linear function of the expansion factor given by $\alpha \equiv (\alpha_0 + \alpha_a(1-a))$, H the Hubble parameter and α_0, α_a dimensionless parameters.

This model also has analytical solution for the reduced model of Eq.(2.78) when $\alpha_a = 0$, then $\alpha = \alpha_0$. We obtain under this assumptions

$$\rho_\Lambda = A\left(A + Ba^{-3(1+\alpha)}\right)^{-\frac{\alpha}{1+\alpha}}, \tag{2.82}$$

$$\rho_c = \left(A + Ba^{-3(1+\alpha)}\right)^{-\frac{1}{1+\alpha}} - \rho_\Lambda, \tag{2.83}$$

where

$$A \equiv \rho_\Lambda^0(\rho_\Lambda^0 + \rho_c^0)^\alpha, \tag{2.84}$$

$$B \equiv \rho_c^0(\rho_\Lambda^0 + \rho_c^0)^\alpha, \tag{2.85}$$

with ρ_c^0, ρ_Λ^0 densities at the present time.

2.6.5 Effective Equation of State for the Interacting Dark Energy

We would like to introduce an indicator of the interacting Dark Energy dynamics. The common equation of state for Dark Energy defined in Eq.(2.52) is not a good indicator because it has no direct information about the Dark Energy density evolution. To solve this issue consider the Friedmann equation for non-interacting Dark Energy

$$\rho'_\Lambda + 3aH(1+w)\rho_\Lambda = 0, \tag{2.86}$$

where the prime denotes derivation respect to conformal time and w is the usual equation of state.

Solving for w and implementing the background equations (2.72), (2.73), and (2.74) we obtain after some simple calculations

$$w_{eff} \equiv -1 - \frac{Q}{3H\rho_\Lambda}. \tag{2.87}$$

Note that w_{eff} is not a formal equation of state for Dark Energy as it mixes interacting and non-interacting models, but it is used because it is proportional to ρ'_Λ and therefore it is a good indicator for the Dark Energy dynamics.

2.6.6 Linear Perturbation Equations

Taking first order perturbation terms of Eqs. (2.68), (2.69), (2.70) and (2.71) we obtain

$$\delta Q^{DM} = -\frac{3a'\delta\rho_c}{a^2} - \frac{(\delta\rho_c)'}{a} + \frac{\rho_c}{a}(-\nabla^2 E' - \nabla^2 v + 3\Psi'), \tag{2.88}$$

$$\delta f_i^{DM} = \frac{\rho_c}{a}(av_{,i})', \tag{2.89}$$

$$\delta Q^{DE} = -\frac{\delta\rho'_\Lambda}{a}, \tag{2.90}$$

$$\delta f_i^{DE} = -\rho'_\Lambda v_{,i} - \delta\rho_{\Lambda,i}, \tag{2.91}$$

where the notation $Q \equiv Q_0 + \delta Q$ and $f_i \equiv f_{i,0} + \delta f_i$ is employed and subscript zero denotes background level.

2.6.6.1 The Dark Matter Geodesic Model

We now must choose a particular model for f_i as we can not infer it from the background level, i. e., at linear perturbation level we have more degrees of freedom. The Dark Matter Geodesic Model [32], states $f_i^{DM} = 0$. That means there is no net force applied over the Dark Matter fluid so it follows geodesics. As we can see in Eq.(2.89), f_i^{DM} is proportional to the time variation of fluid velocity v and therefore we can identify f_i with a force or at least proportional to it. So adopting this model, from Eq.(2.89) and defining $\theta_i \equiv a v_{,i}$ we have

$$\theta_i' = 0. \tag{2.92}$$

Also in synchronous gauge we can set $\theta_{ini} = 0$ so from Eq.(2.92) we infer

$$\theta_i = 0, \quad for \quad all \quad times. \tag{2.93}$$

On the other hand if $f_i^{DM} = 0$ then Eq.(2.59) implies $f_i^{DE} = 0$, and from Eq.(2.91) we obtain

$$a\delta\rho_{\Lambda,i} = -\theta_i \rho_\Lambda'. \tag{2.94}$$

The statement of Eq.(2.93) implies from Eqs.(2.94) and (2.90)

$$\delta\rho_{\Lambda,i} = 0, \tag{2.95}$$

$$\delta Q^{DE} = 0. \tag{2.96}$$

So in the Dark Matter Geodesic Model and in synchronous gauge the only remaining equation for perturbations is Eq.(2.68) and reduces to

$$\delta Q \equiv \delta Q^{DM} = -\frac{3a'\delta\rho_c}{a^2} - \frac{(\delta\rho_c)'}{a} + \frac{\rho_c}{a}(-\nabla^2 E' + 3\Psi'). \tag{2.97}$$

We can rewrite Eq.(2.97) using Eqs.(2.73), (2.74) and introducing the definitions

$$\delta_c \equiv \frac{\delta\rho_c}{\rho_c}, \tag{2.98}$$

$$h \equiv 2(\nabla^2 E - 3\Psi). \tag{2.99}$$

So we finally obtain the unique and reduced equation for linear perturbations in synchronous gauge and in Dark Matter Geodesic Model

$$\delta_c' = \frac{aQ\delta_c}{\rho_c} - \frac{h'}{2}. \tag{2.100}$$

2.6.7 Adiabatic Initial Conditions

In order to solve numerically the perturbation equation (2.100), we need to know about initial conditions of primordial perturbations. In a first attempt let us assume that the primordial perturbations can be described by only one degree of freedom and that the Universe is compose with a mixture of non-interacting perfect fluids which background quantities evolution is known. In that situation we can expand at first order for a generic x component of the Universe

$$\rho_x(\eta, \mathbf{x}) = \overline{\rho}_x(\eta + \delta\eta(\mathbf{x})) \simeq \overline{\rho}_x(\eta) + \overline{\rho}'_x(\eta)\delta\eta(\mathbf{x}), \tag{2.101}$$

$$p_x(\eta, \mathbf{x}) = \overline{p}_x(\eta + \delta\eta(\mathbf{x})) \simeq \overline{p}_x(\eta) + \overline{p}'_x(\eta)\delta\eta(\mathbf{x}), \tag{2.102}$$

where as usual η is the conformal time and primes indicates derivative respect to η.

We can see in this expansion that the evolution of primordial perturbations is given by a homogeneous cosmology plus an evolution proportional to the single degree of freedom $\delta\eta(\mathbf{x})$ that can be seen as a time shifting function and also proportional to the known background quantities derivatives $\overline{\rho}'_x$ and $\overline{p}'_x$.

The assumptiom of adiabatic initial conditions (2.101) and (2.102) led to the useful relation for any x or y component of the Universe

$$\frac{\delta p_x}{\overline{\rho}_x + \overline{p}_x} = \frac{\delta p_y}{\overline{\rho}_y + \overline{p}_y}. \tag{2.103}$$

If we consider for example a Universe containing only photons, baryons, Cold Dark Matter and neutrinos we can infer using that for non-relativistic species $\overline{p} \ll \overline{\rho}$ and for ultra-relativistic ones we have $\overline{p} = \overline{\rho}/3$ therefore we obtain using Eq.(2.103)

$$\delta_b = \delta_c = \frac{3}{4}\delta_\nu = \frac{3}{4}\delta_\gamma, \tag{2.104}$$

where the generic dimensionless parameter $\delta_x \equiv \delta\rho/\overline{\rho}_x$ is used.

Moreover we can obtain the relation for the total perturbation

$$\delta p_{total}(\eta, \mathbf{x}) = c_s^2(\eta)\delta p_{total}(\eta, \mathbf{x}), \tag{2.105}$$

with c_s the adiabatic sound speed of the total composed fluid which actually is a weighted average over the different sound speeds of each component. The fact that this adiabatic sound speed exists is the reason why Eqs.(2.101) and (2.102) are called adiabatic initial conditions.

2.7 Usage of Newtonian Gauge in this section

For pedagogical purposes this section will be derived in Newtonian Gauge where we will explain the physics of CMB anisotropies in terms of potentials Ψ and ϕ.

One advantage of working in Newtonian Gauge is that the δG^i_j Einstein equation is

$$\frac{2}{3}\left(\frac{k}{a}\right)^2(\phi-\Psi)=8\pi G\sum_x(\overline{\rho}_x+\overline{p}_x)\sigma_x, \tag{2.106}$$

with σ_x the anisotropic stress of a generic x component of the Universe. If we consider that all components of the Universe can be modeled as a perfect fluid we will have $\sigma_x=0$ for all x, and as a consequence

$$\phi=\Psi. \tag{2.107}$$

If we focus on the radiation dominated era and replace Eq.(2.107) in Einstein equations, one can find a second order differential equation for Ψ only and can show [33] that it has two solutions; one decaying and one constant in time that reads in combination with Eq.(2.104)

$$-2\phi=-2\Psi=\delta_{total}\simeq\delta_\gamma=constant, \tag{2.108}$$

therefore under all these assumptions the metric fluctuations are static. This holds even in the matter domination era but in that case we would have $\delta_{total}\simeq\delta_b=(3/4)\delta_\gamma$.

2.7.1 Power Spectrum and Transfer Functions

The theory of cosmological perturbations is a stochastic one, this means that for some given fluctuations $A(\eta,\mathbf{x})$ of a quantity in a given point there exists a probability distribution that describes the situation. As long as we are dealing with linear perturbations this probability can be considered to scale also linearly. And is well known that if we suppose this probability distribution to be Gaussian it will remain Gaussian at all times. In this sense the study of the evolution of the perturbations reduces to study the evolution of its statistical averages that here will be denoted with angled brackets $\langle\ \rangle$.

Now we introduce the two point and equal-time correlation function

$$\langle A(\eta,\mathbf{x}),A(\eta,\mathbf{x'})\rangle\equiv\xi(\eta,\mathbf{x},\mathbf{x'})=\xi(\eta,|\mathbf{x}-\mathbf{x'}|), \tag{2.109}$$

where the last equality lies on the assumption of Statistical Homogeneity and Isotropy that is expected to hold in the linearly perturbed Universe.

If $A(\eta, \mathbf{x})$ is real and we use the same letter A to denote the fourier transform of A we can obtain the relation

$$\langle A(\eta, \mathbf{k}), A(\eta, \mathbf{k'}) \rangle = \delta_D(\mathbf{k} - \mathbf{k'}) P_A(k), \tag{2.110}$$

here δ_D is the Dirac delta function and SHI causes the correlation function vanish for $\mathbf{k} \neq \mathbf{k'}$ and that P_A is a function of $k = |\mathbf{k}|$.

The function P_A is called the Power Spectrum of A. Recall from Eq.(2.104) that perturbations are strongly related, so we only need to specify one Power Spectrum in order to know all the others

$$P_b = P_c = \frac{9}{16} P_\nu = \frac{9}{16} P_\gamma. \tag{2.111}$$

In Newtonian gauge is common to define the Primordial Spectrum in terms of the variable

$$R \equiv \Psi - \frac{1}{3} \frac{\delta \rho_{total}}{\overline{\rho}_{total} + \overline{p}_{total}}, \tag{2.112}$$

which describes the spatial curvature perturbation on one initial comoving hypersurface and has the property of being conserved on scales comparable to the Hubble radius or larger [34]. This is important because in an early stage of the Universe we can consider that most Fourier modes of primordial perturbations are outside the Hubble radius. Hence, the perturbations evaluated at some arbitrary time but on super-Hubble scales reflect directly the mechanism responsible for the formation of perturbations in the early Universe.

We can split the Power Spectrum of A in two parts

$$P_A(k) = \left[\frac{A(\eta, \mathbf{k})}{R(\mathbf{k})} \right]^2 P_R(k), \tag{2.113}$$

where the function

$$A(\eta, k) \equiv \left[\frac{A(\eta, \mathbf{k})}{R(\mathbf{k})} \right], \tag{2.114}$$

is known as the Transfer Function of A. Note that we have used the same letter for the fluctuation $A(\eta, \mathbf{k})$ and for the transfer function $A(\eta, k)$, the difference is that the former depends on $\mathbf{k}$ and the latter only on k.

These transfer functions describe the linear evolution of the perturbations and are to be known in order to evolve the statistical averages of the diverse quantities.

2.7.2 The CMB Power Spectrum

In a first instance we can consider a primordial and coupled system of baryons, electrons and photons at a very early stage of the Universe. Electrons and baryons interact via electromagnetic forces since they carry opposite electric charges, baryons and photons principal interaction is the gravitational one. Meanwhile electrons and photons interact via Thompson scattering, understood as the limit of Compton scattering when the electrons are not relativistic and the photons have less energy than the rest mass of the electron.

The Thomson scattering rate with respect to conformal time is

$$\Gamma = \sigma_T a n_e \chi_e, \tag{2.115}$$

with σ_T the Thomson scattering surface, a the expansion factor, n_e the electron number density and χ_e the ionized electron fraction. Note that $n_e \sim 1/a^3$ due to the dilution and that $\chi_e \sim 1$ at high energies. Then, at the recombination epoch when the electrons and nuclei begin to form atoms $\chi_e \to 0$. For this reasons Thomson scattering becomes inefficient and photon decouple from the system.

Some useful parameters are defined below.

The **optical depth** that represents the opacity of the Universe at a given time when seen today (η_0)

$$\tau(\eta) \equiv \int_{\eta}^{\eta_0} d\eta \Gamma(\eta). \tag{2.116}$$

The **visibility function** gives the probability that a CMB photon seen today experienced its last scattering at time η

$$g(\eta) \equiv -\tau' e^{-\tau}. \tag{2.117}$$

The **diffusion length** λ_d can be known through the mean free-path of photons $r_{mfp} = \Gamma^{-1}$, then the comoving distance they travel between η_{ini} and η is approximately

$$r_d \simeq \left[\int_{\eta_{ini}}^{\eta} d\eta \Gamma r_{mfp}^2\right]^{\frac{1}{2}} = \left[\int_{\eta_{ini}}^{\eta} d\eta \Gamma^{-1}\right]^{\frac{1}{2}}, \tag{2.118}$$

Then the diffusion length can be computed

$$\lambda_d = a r_d. \tag{2.119}$$

The **sound horizon at decoupling** $d_s(\eta_{dec})$ is the distance traveled by a wavefront between some initial time in the primordial Universe and the time of photon decoupling

$$d_s = a \int_{\eta_{ini}}^{\eta} c_s d\eta, \tag{2.120}$$

with c_s the sound speed in the photon-baryon fluid. Note that two points on the last scattering surface separated this distance should be partially correlated since density wave have propagated from one point to the other. This will be important when studying the features of CMB power spectrum at angular scales corresponding at sound speed at decoupling.

2.7.3 CMB anisotropies

At a first look the CMB radiation seems to be the same in all directions. Decades after its discovering irregularities were measured from looking at different directions, which were hard to detect because they are of order $10^{-4}K$. This anisotropies are important because they contain information about decoupling epoch.

In order to study these anisotropies, first consider again the primordial and coupled system of photons, baryons and electrons in the very early Universe. In this scenario the highly coupled system can be considered in thermal equilibrium, so the phase space distribution of photons corresponds to the Bose-Einstein distribution

$$f(\eta, \mathbf{x}, \mathbf{p}) = \frac{1}{e^{\frac{p}{T(\eta,\mathbf{x})}} - 1}. \tag{2.121}$$

Expanding at first order in perturbations $f = \overline{f} + \delta f$ we can obtain

$$\overline{f}(\eta, p) = \frac{1}{e^{\frac{p}{\overline{T}(\eta)}} - 1} \tag{2.122}$$

$$\delta f = \frac{d\overline{f}}{d\log p} \frac{\delta T(\eta, \mathbf{x})}{\overline{T}(\eta)}. \tag{2.123}$$

From the above expressions we see that is feasible to characterize CMB anisotropies at first order in perturbations with the function

$$\Theta(\eta, \mathbf{x}) \equiv \frac{\delta T(\eta, \mathbf{x})}{\overline{T}(\eta)}. \tag{2.124}$$

Note that we observe in practice the temperature in a given direction $\hat{\mathbf{n}}$, at actual time $\eta = \eta_0$ and at a fixed location $\mathbf{x} = \mathbf{o}$, so we can consider in local spherical coordinates

$$\Theta_{obs} = \Theta(\eta_0,\ \mathbf{o},\ \hat{\mathbf{n}}) = \Theta(\hat{\mathbf{n}}) = \Theta(\theta, \phi). \tag{2.125}$$

Therefore expanding in spherical harmonics $Y_m^\ell(\theta, \phi)$ is feasible

$$\Theta_{obs}(\theta, \phi) = \sum_\ell \sum_m a_{\ell m} Y_m^\ell(\theta, \phi). \tag{2.126}$$

Then, the coefficients $a_{\ell m}$ give information about anisotropies on various scales.

In the Fourier space the dependency $\Theta_{obs} = \Theta(\eta,\ \mathbf{k},\ \hat{\mathbf{n}})$ can be changed to $\Theta_{obs}(\eta, k, \theta)$. Recall that in a Fourier transform we perform a decomposition in plane waves and at that level all that matters is the product $\mathbf{k} \cdot \mathbf{n} = kcos\theta$ at the local point of observation. Also the plane waves carry azimuthal symmetry, so we can perform the expansion

$$\Theta_{obs}(\eta, k, \theta) = \sum_\ell (-i)^\ell (2\ell + 1)\Theta_\ell(\eta, k) P_\ell(cos\theta). \tag{2.127}$$

Using the above expansions and some relations between spherical harmonics and Legendre polynomials we can obtain

$$a_{\ell m} = (-i)^\ell \int \frac{d^3\mathbf{k}}{2\pi^2} Y_{\ell m}(\theta, \phi)\Theta_\ell^2(\eta, k). \tag{2.128}$$

Defining now the radiation angular power spectrum C_ℓ is straightforward with the aid of orthogonality relations of spherical harmonics and it is convenient to put it in terms of the primordial spectrum $P_R(k)$

$$C_\ell \equiv \left\langle |a_{\ell m}|^2 \right\rangle = \frac{1}{2\pi^2} \int \frac{dk}{k} \Theta_\ell^2(\eta_0, k) P_R(k), \tag{2.129}$$

where the angled brackets denote statistical average, i.e., an average over all possible observers in the Universe. The independence of the angular power spectrum on the index m comes from the fact that we can only study radiation that comes to the Earth ignoring all remaining information from radiation arriving other locations, so all we can do is an average over index m. Furthermore, the statistical results require rotational invariance, so the power spectrum only depends on index ℓ, telling us about the angular scales in the anisotropies. Roughly speaking the index ℓ gives us information of a scale $180°/\ell$. Note that the term associated to $\ell = 0$ is a constant because of the spherical harmonics's properties and as a consequence statistically is not important. Meanwhile

$\ell = 1$ gives the difference in temperature from opposite sides of the sky and is believed to arise from the relative motion between the Earth and the CMB radiation causing a Doppler effect. So the CMB angular power spectrum is often reported from $\ell > 2$ since the other values do not carry intrinsic information about the cosmic background radiation.

2.7.4 Physics of the CMB Power Spectrum

In this section we will make a descriptive discussion of the physical phenomena that the CMB power spectrum contains, in order to obtain the physical information of our results. For further information and intermediate steps see for example [33].

Recall that for a generic function we have

$$\frac{dF(\eta, \mathbf{x}, \hat{\mathbf{n}})}{d\eta} = F' + \frac{dx_i}{d\eta}\frac{\partial F}{\partial x_i} + \frac{dn_i}{d\eta}\frac{\partial F}{\partial n_i}. \tag{2.130}$$

If we consider photons traveling approximately in a straight line $\frac{dn_i}{d\eta} \approx 0$ and at the speed of light along our line of sight $\hat{\mathbf{n}}$. We then have $\frac{dx_i}{d\eta} = \hat{\mathbf{n}}$ and the above expression reduces to

$$\frac{dF(\eta, \mathbf{x}, \hat{\mathbf{n}})}{d\eta} = F' + \hat{\mathbf{n}} \cdot \nabla F. \tag{2.131}$$

In the Newtonian gauge, choosing $F(\eta, \mathbf{x}, \hat{\mathbf{n}}) = e^{-\tau(\eta)}(\Theta(\eta, \mathbf{x}, \hat{\mathbf{n}}) + \Psi(\eta, \mathbf{x}))$, with $\tau(\eta)$ the optical depth defined in Eq.(2.116) and integrating along the line of sight we can obtain with aid of the visibility function g defined in Eq.(2.117)

$$(\Theta + \Psi)\mid_{obs} = \int_{\eta_{ini}}^{\eta_0} d\eta \bigg(g(\Theta_0 + \Psi + \hat{\mathbf{n}} \cdot \mathbf{v}_b) + e^{-\tau}(\phi' + \Psi') \bigg), \tag{2.132}$$

with Θ_0 the monopole contribution to temperature anisotropies (the average of Θ over all directions $\hat{\mathbf{n}}$) and $\mathbf{v}_b$ the velocity of baryons (that in the highly coupled regime equals the velocity of photons).

Assuming the instantaneous decoupling approximation, where all photons decouple precisely at the time η_{dec}, we can replace the visibility function with a Dirac Delta and the the exponential with a Heaviside function and obtain

$$\Theta\mid_{obs} = (\Theta_0 + \Psi)\mid_{dec} + \hat{\mathbf{n}} \cdot \mathbf{v}_b \mid_{dec} + \int_{\eta_{dec}}^{\eta_0} d\eta(\phi' + \Psi'), \tag{2.133}$$

where we have neglected the $\Psi|_{obs}$ in the left hand side of the above expression, since it contributes only with a minimal correction to the anisotropies and in practice it is not measurable.

We can perform a similar analysis in the Fourier space and compute the contributions of each term to the power spectrum C_ℓ, obtaining the three following contributions

$$C_\ell^{SW} \sim \langle|\Theta_0 + \Psi|^2\rangle \quad at \quad (\eta, k) \simeq \left(\eta_{dec}, \frac{\ell}{\eta_0 - \eta_{dec}}\right), \tag{2.134}$$

$$C_\ell^{Doppler} \sim \langle|\theta_b|^2\rangle \quad at \quad (\eta, k) \simeq \left(\eta_{dec}, \frac{\ell}{\eta_0 - \eta_{dec}}\right), \tag{2.135}$$

$$C_\ell^{ISW} \sim \langle|\phi' + \Psi'|^2\rangle \quad for\ all \quad (\eta, k) \simeq \left(\eta_{dec}, \frac{\ell}{\eta_0 - \eta}\right), \tag{2.136}$$

note that the power spectrum approximately encodes information for a subtended angle on the last scattering surface $\theta = \pi/\ell$, which corresponds to a physical scale θd_{ang}, with d_{ang} the diameter angular distance previously defined. For photons traveling in a radial trajectory toward us, the diameter angular distance simplifies a lot. And this corresponds to a wavenumber k such that

$$\frac{\pi a(\eta_{dec})}{k} = \theta d_{ang} = \frac{\pi}{\ell} a(\eta_{dec}) \int_{\eta_{dec}}^{\eta_0} d\eta = \frac{\pi}{\ell} a(\eta_{dec})(\eta_0 - \eta_{dec}), \tag{2.137}$$

from where follows the relation $k \simeq \frac{\ell}{\eta_0 - \eta}$.

This contributions are often called the Sachs-Wolfe (SW), the Doppler and the Integrated Sachs-Wolfe (ISW) contributions respectively.

2.7.4.1 The Sachs-Wolfe Contribution

This term essentially depends on the value of $\Theta_0\,|_{dec}$ and $\Psi\,|_{dec}$ on one point on the last scattering surface at the instantaneous decoupling time η_{dec}. We can interpret $\Theta_0\,|_{dec}$ as an intrinsic temperature and $\Psi\,|_{dec}$ as a gravitational Doppler shift.

We now turn our attention to the $\Theta_0\,|_{dec}$ term.

In the highly coupled regime the electrons, baryons and photons form an effective single fluid with adiabatic sound speed

$$c_s = \frac{\delta p_\gamma + \delta p_b + \delta p_e}{\delta\rho_\gamma + \delta\rho_b + \delta\rho_e} \simeq \frac{\delta p_\gamma}{\delta\rho_\gamma + \delta\rho_b}, \tag{2.138}$$

since $\delta p_e, \delta p_b \ll \delta p_\gamma$. We can further simplify this expression considering local values of temperature. We know from thermodynamics that $\rho_b \propto T^3$ and $\rho_\gamma \propto T^4$, this implies $\delta_\gamma = \frac{4}{3}\delta_b$. So we obtain

$$c_s^2 = \frac{1}{3(1+X)}, \quad X \equiv \frac{\rho_b}{\rho_\gamma}. \tag{2.139}$$

It is possible to derive and equation of motion for Θ_0 in the tightly-coupled regime

$$\Theta_0'' + \frac{X'}{1+X}\Theta_0' + k^2 c_s^2 \Theta_0 = -\frac{k^2}{3}\Psi + \frac{X'}{1+X}\phi' + \phi''. \tag{2.140}$$

Eq.(2.140) is very illustrative because without need of solving it we can infer qualitatively the behavior of $\Theta_0(k)$. First we note that if X were constant in time and if we did not have gravitational perturbations ($\phi = \Psi = 0$) this equation would reduce to that of a harmonic oscillator with solution

$$\Theta_0 = \Theta_{ini} cos(k c_s \eta + \varphi). \tag{2.141}$$

Now it is convenient to recall Eq.(2.120) where we defined the sound horizon, for the case of a constant sound speed this reduces to $d_s = a c_s \eta$. So, the condition $k c_s \eta \ll 1$ corresponds to $\lambda \gg d_s$, for the physical wavelength $\lambda = 2\pi a/k$. This is important because we conclude for k_s (the corresponding wavenumber of d_s), that Θ_0 is approximately constant for $k < k_s$ since the cosine argument is negligible and then it begins to oscillate for $k > k_s$.

Another important characteristic is that we can find the equilibrium point or zero-point of oscillation by putting in a first approach $\Theta_0'' = \Theta_0' = \phi' = \phi'' = 0$ in Eq.(2.140) finding

$$\Theta_0^{equilibrium} \simeq -(1+X)\Psi. \tag{2.142}$$

We can find in the literature [33] that the fluctuation $\Psi(k) \to 0$ as k increases. Also we know from Eq.(2.108) that for early stages of the Universe where $\eta \ll 1$ and therefore $k c_s \eta \ll 1$, the metric fluctuations are frozen. Then Ψ can be considered constant for $k < k_s$.

If we now take the SW contribution to the power spectrum $(\Theta_0 + \Psi)\,|_{dec}$ we can see that there are three principal regions of evolution of this sum of functions.

- Region I ($k < k_s$). In this region both Ψ and Θ_0 are constant so $(\Theta_0 + \Psi)\,|_{dec}$ is constant. This region is often called the Sachs-Wolfe Plateau.

- Region II ($k \approx k_s$). Here Θ_0 begins to oscillate. The first peak is enhanced by gravitational forces that favor the formation of over-densities and a subsequent negative peak in the temperature fluctuations (Recall $-2\Psi = \delta_{tot} \simeq \delta_b = \frac{3}{4}\delta_\gamma = 3\Theta_0$). We also have to add the contribution of the changing zero-point of oscillations $-(1+X)\Psi$ that vanishes as k increases, this contributes only to odd-peaks since they are all negatives, and reduces even-peaks as they carry opposite sign.

- Region III ($k \gg k_s$). This region is characterized by the fact that since k is large, then λ is small. And in a extreme situation this wavelength could be comparable to the microscopic scales on the primordial plasma. And in that case we could not apply a fluid description of the system. So Eq.(2.140) does not hold in this region. But we can infer that as frecuency is large, since λ is small, the more cycles made, the more damping experienced. This damping is governed by the diffusion length λ_d defined in Eq.(2.119) and can be proved that the envelope of peaks is proportional to $e^{-(k/k_d)^2}$, with k_d the corresponding wavenumber of λ_d. So damping effect is greater for k large.

2.7.4.2 The Doppler Contribution

This is the contribution to the power spectrum of standard Doppler effect and it is related to $\langle|\theta_b|^2\rangle$ at decoupling. We can prove that this contribution is proportional to Θ_0' and then from basic acoustic oscillation theory we know that if Θ_0 oscillates then Θ_0' will also oscillate but with a different phase. We can split this contribution in the regions

- Region I ($k < k_s$). We know that in this region $\Theta_0' = 0$ since Θ_0 is constant. Therefore the Doppler contribution is null in this region.

- Region II ($k > k_s$). This contribution oscillates out of phase respect to Θ_0.

2.7.4.3 The Integrated Sachs-Wolfe Contribution

We know that this contribution depends strongly in the temporal variation of the metric fluctuations ϕ' and Ψ'. This quantities are principally important when the Universe changes its expansion rate, for example in the radiation-matter equality epoch or more recently in the matter-Dark Energy equality epoch. This in practice means that the

first transition will have a contribution to the power spectrum about the first peak and the second transition will affect small values of ℓ causing a tilt in the Sachs-Wolfe plateau.

2.7.5 Parameter dependence in the CMB Power Spectrum

It is common to define the Primordial spectrum as

$$P_R(k) \equiv A_s \left(\frac{k}{k_*}\right)^{n_s-1}, \tag{2.143}$$

with A_s the spectrum amplitude, k_* an arbitrary fixed wavenumber scale and n_s the spectral index or tilt of the spectrum.

We can choose a six parameter basis in analogy to ΛCDM model. There are several options but assuming a flat Universe we will choose the parameter basis

$$\{A_s,\ n_s,\ \Omega_\Lambda,\ \Omega_m,\ \Omega_b,\ \tau_{reio}\}, \tag{2.144}$$

with τ_{reio} the optical depth at reionization.

Now we can identify the principal characteristics of the CMB Power Spectrum in the ΛCDM model and relate them to the corresponding parameters of the basis.

I. Global Amplitude $\rightarrow$ A_s.

II. Global tilt $\rightarrow$ n_s.

III. First peak scale $\rightarrow$ $\Omega_\Lambda,\ \Omega_m,\ \Omega_b$.

IV. Ratio of odd-even peaks $\rightarrow$ Ω_b.

V. Amplitude of first peaks $\rightarrow$ Ω_m.

VI. Damping envelope $\rightarrow$ $\Omega_\Lambda,\ \Omega_m,\ \Omega_b$.

VII. Sachs-Wolfe plateau tilting $\rightarrow$ Ω_Λ.

VIII. Amplitude for $\ell > 40$ $\rightarrow$ τ_{reio}.

This will become important when we analyze the CMB Power Spectrum for the interacting model, where we will have and extended basis depending on the parameters of a particular interacting model.

2.7.6 Parameter Basis in the Interacting Models

We have to add to the ΛCDM parameter basis the corresponding parameters of each interacting model.

Recall interacting functions definitions Eqs.(2.76), (2.77), (2.81). Then, we will have the following parameter basis for the interacting models

- For Constant interacting model $\{A_s,\ n_s,\ \Omega_\Lambda,\ \Omega_m,\ \Omega_b,\ \tau_{reio},\ Q_0\}$
- For Martinelli's interacting model $\{A_s,\ n_s,\ \Omega_\Lambda,\ \Omega_m,\ \Omega_b,\ \tau_{reio},\ q_0\}$
- For Wang's interacting model $\{A_s,\ n_s,\ \Omega_\Lambda,\ \Omega_m,\ \Omega_b,\ \tau_{reio},\ \alpha_0,\ \alpha_a\}$

2.8 The Matter Power Spectrum

We can characterize the fluctuations in matter density at position $\mathbf{x}$ relative to the average density $\overline{\rho}$ with the dimensionless function

$$\delta(\mathbf{x}) \equiv \frac{\rho(\mathbf{x}) - \overline{\rho}}{\overline{\rho}}. \tag{2.145}$$

The Matter Power Spectrum is understood as the Fourier transform of the auto-correlation function ξ, defined by

$$\xi(r) \equiv \left\langle \delta(\mathbf{x})\delta(\mathbf{x}') \right\rangle, \tag{2.146}$$

where angled brackets stands for average over all space and $r = |\mathbf{x} - \mathbf{x}'|$. So we have the relation for the Matter Power Spectrum $P(k)$

$$\xi(r) = \int \frac{d^3k}{(2\pi)^3} P(k) e^{i\mathbf{k}\cdot(\mathbf{x}-\mathbf{x}')}. \tag{2.147}$$

In this sense if $\xi(r)$ gives the probability of finding matter given a distance r, then the Matter Power Spectrum decomposes this probability into characteristic lengths L, with $k \approx 2\pi/L$.

If $\tilde{\delta}(\mathbf{k})$ is the Fourier transform of $\delta(\mathbf{k})$, we find the useful relation averaging over Fourier space

$$\left\langle \tilde{\delta}(\mathbf{k})\tilde{\delta}(\mathbf{k}') \right\rangle = (2\pi)^3 P(k)\delta^3(\mathbf{k} - \mathbf{k}'), \tag{2.148}$$

where δ^3 is the Dirac Delta function.

3

Metodology

Here we present in Fig.(3.1) the global procedure carried out in this work. Subsequent sections expand the information about each stage.

3.1 The Cosmic Linear Anisotropy Solving System (CLASS)

3.1.1 Overview of CLASS

CLASS is a free provided and C language based program whose purpose consists in computing some background quantities, thermodynamical quantities, perturbation transfer functions, and finally power spectra for a given set of cosmological parameters. Here we present a brief overview, but further information can be found in the CLASS official manual [9]. This task is done basically in ten steps associated to one of the ten modules (modulename.c).

1. Set input parameter values. (input.c)
2. Compute the evolution of cosmological background quantities. (background.c)
3. Compute the evolution of thermodynamical quantities. (thermodynamics.c)
4. Compute the evolution of source functions by integrating over all perturbations. (perturbations.c)
5. Compute the primordial spectra. (primordial.c)
6. Compute non-linear corrections at small redshift.(nonlinear.c)

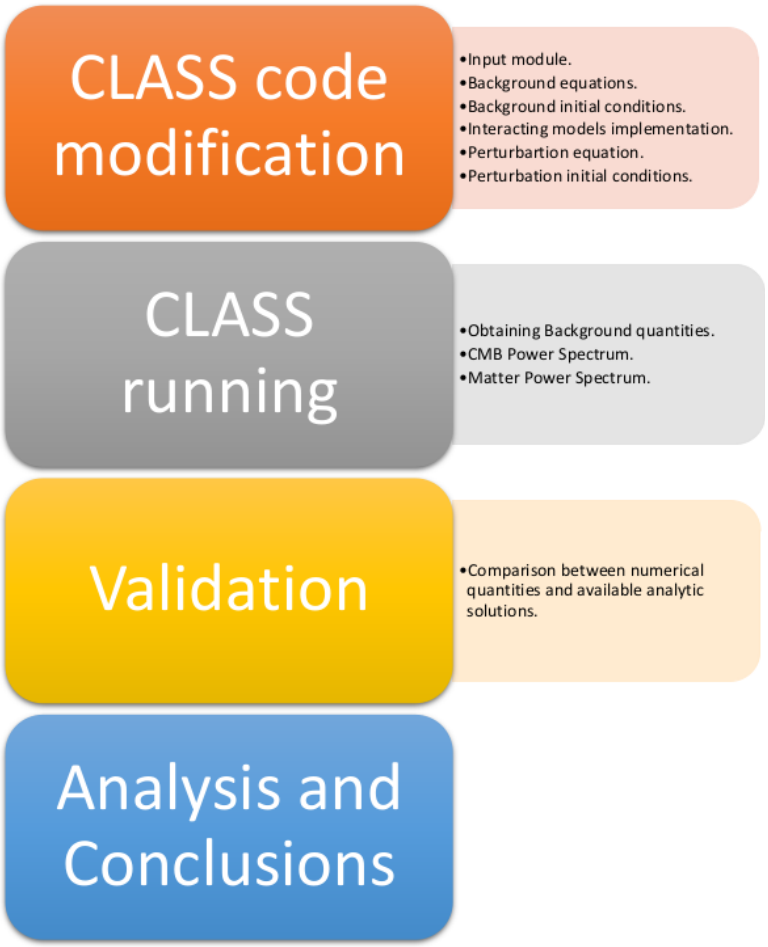

Figure 3.1: Metodology - Block diagram containing the general procedure of this work.

7. Compute transfer functions in harmonic space. (transfer.c)
8. Compute the observable power spectra C_ℓ by convolving the primordial spectra and the harmonic transfer functions and compute matter power spectrum $P(k)$ by multiplying the primordial spectra and the appropriate source functions. (spectra.c)
9. Compute the lensed CMB spectra. (lensing.c)
10. Write results in files. (output.c)

3.2 Implementing the Dark Energy- Dark Matter Model in CLASS

CLASS classifies parameters in three general cases

- $\{A\}$, which can be expressed directly as functions of some parameters $\{B\}$
- $\{B\}$, which need to be integrated over conformal time through first order differential equations.
- $\{C\}$, which also need to be integrated but are not used to compute $\{A\}$

For example for ΛCDM model

- $\{A\} = \{\rho_i(a), p_i(a), H(a), ..., \}$.
- $\{B\} = \{a\}$.
- $\{C\} = \{t, ..., \}$

Another example is extended cosmology with a scalar field ϕ

- $\{A\} = \{\rho_i(a), p_i(a), H(a), ..., V(\phi), ..., \}$
- $\{B\} = \{a, \phi\}$

The last example is important because in this work we followed the structure of a cosmology with a scalar field ϕ, making the identifications

- $V \longrightarrow Q$,

- $\phi \longrightarrow \rho_{\Lambda,int}, \rho_{c,int},$

since we noticed that Q is an $\{A\}$ parameter and ρ_Λ, ρ_c are $\{B\}$ parameters in the interacting model. We can explicitly see this in the background equations (2.72), (2.73) and (2.74).

3.2.1 The shooting method

The shooting method in numerical analysis is a method that changes a boundary value problem to an initial conditions problem. It suits our situation because we know which are the present values of density parameters Ω_c^0 and Ω_Λ^0, but initial conditions are in general not known. In that sense we have fixed values for Ω_c^0 and Ω_Λ^0 which can be seen as targets and we are looking for initial values that evolved via numerical integration hit the targets. The process can be divided in the following steps.

- CLASS code reads as inputs the values of targets and some proposed values that we named in the code `omega0l_prop` and `omega0m_prop`. They are also known as shooting parameters.

- CLASS needs functions that relate the initial conditions ρ_c^{ini} and ρ_Λ^{ini} with their respective shooting parameter. A standard proposal is to use the solution for ΛCDM,

$$\rho_\Lambda^{ini} = \Omega_{\Lambda,prop}^0 H_0^2, \tag{3.1}$$

$$\rho_c^{ini} = \Omega_{c,prop}^0 H_0^2 \left(\frac{a_0}{a_{ini}}\right)^3. \tag{3.2}$$

  If analytical solutions for a particular interacting model at background level are known, they would be a better choice. But in general this does not happen.

- Initial conditions are computed given the shooting parameters.

- The code integrates numerically the background equations given the initial conditions of the previous step.

- CLASS checks if the numerical solution hits the targets at present time. If so, shooting process is complete; if not the shooting parameters are slightly changed and the process is repeated.

3.3 Modifying CLASS Code

In the next subsections we will present modifications of the input, background and perturbations modules, there are another modifications as definitions of internal variables or indexes, internal checkings of physical congruence for computed quantities, screen warnings to the user, among others. But here we present only the essential parts of the modification of the code.

3.3.1 Modifying Input Module

CLASS has an archive with extension `.ini` which contains a complete set of input parameters for a given cosmology. We had to modify this module in order to input the parameters of our model, that we called `int_parameters`. We also defined a parameter

$$\Omega_{int} \equiv \Omega_c + \Omega_\Lambda, \tag{3.3}$$

that we used as a target instead of Ω_Λ.
First we added the targets and shooting parameters of our model to the existing list of shooting and target parameters in CLASS.

```
char * const target_namestrings[] = {"100*theta_s","Omega_dcdmdr","
   omega_dcdmdr","Omega_scf","Omega_ini_dcdm",
"omega_ini_dcdm","sigma8","Omega_int","omega0m_target"};
 char * const unknown_namestrings[] = {"h","Omega_ini_dcdm","
   Omega_ini_dcdm","scf_shooting_parameter",
 "Omega_dcdmdr","omega_dcdmdr","A_s", "omega0l_prop","omega0m_prop"};
```

Then we added the instruction to read them in the archive with extension `.ini`.

```
class_call(parser_read_double(pfc,"Omega_int",&param5,&flag5,errmsg),
               errmsg, errmsg);
class_call(parser_read_double(pfc,"omega0c_target",&param4,&flag4,errmsg),
               errmsg, errmsg);
```

An important feature of CLASS is that we can choose the contribution of some component as free parameter. We can do this by putting for example $\Omega_{int} < 0$ and in that case CLASS takes Ω_{int} as unspecified and uses it to fulfill the closure relation

$$\sum_{i \in \{all\ species\}} \Omega_i = 1. \tag{3.4}$$

This can be done with an internal checking named `class_test`, here `flag1` refers to Dark Energy as a cosmological constant, `flag2` refers to Dark Energy as a fluid with some equation of state, and our case `flag5` refers to the interacting Dark Energy. The following instruction states that one of this options must be left unspecified in order to fulfill the closure relation.

```
class_test((flag1 == _TRUE_) && (flag2 == _TRUE_) && ((flag5 == _FALSE_)
    || (param5 >= 0.)), errmsg,
"In input file, either Omega_Lambda or Omega_fld must be left unspecified,
    except if Omega_int is set and <0.0, in which case the contribution
   from the interacting fluid will be the free parameter.");

```

If we put for example $0 \leq \Omega_{int} < 1$ this will be simply added to the total density parameter. But if we set it negative, it will be used as free parameter.

```
 if ((flag5 == _TRUE_) && (param5 >= 0.)){
    pba->Omega0_int = param5;
    Omega_tot += pba->Omega0_int;
                                          }
    else if ((flag5 == _TRUE_) && (param5 < 0.)){
    // Fill up with interacting fluid
    pba->Omega0_int = 1. - pba->Omega0_k - Omega_tot;
    if (input_verbose > 0) printf(" -> matched budget equations by
    adjusting Omega_int = %e\n",pba->Omega0_int);
```

The following definition of `Omega0_int` is important because we are taking this as a target with shooting parameter `omega0l_prop`. This can be seen explicitly in the following instruction where the difference between targets and numerical quantities are made. If this difference in close enough to zero the shooting is completed, if not the shooting process repeats. [1]

```
case Omega_int:
  output[i] = (ba.background_table[(ba.bt_size-1)*ba.bg_size+ba.
    index_bg_rho_c_int]+ba.background_table[(ba.bt_size-1)*ba.bg_size+ba.
    index_bg_rho_l_int])/(ba.H0*ba.H0)-ba.Omega0_int;
            break;
case omega0m_target:
  output[i] = (ba.background_table[(ba.bt_size-1)*ba.bg_size
             +ba.index_bg_rho_c_int])/(ba.H0*ba.H0)-ba.omega0m_target;
        break;
```

[1] Note for example that an internal way to call the computed ρ_c is `(ba.background_table[(ba.bt_size-1)*ba.bg_size+ba.index_bg_rho_c_int])`.

The rest of the modifications in the input module only read in the `.ini` file the parameters needed for our model.

- `int_parameters`: Includes the parameters for a particular interacting model and shooting parameters.
- `int_parameters_size`: Defines the number of parameters.

```
if (pba->Omega0_int != 0.){
    class_call(parser_read_list_of_doubles(pfc, "int_parameters",
    &(pba->int_parameters_size),&(pba->int_parameters),&flag1,errmsg),
    errmsg,errmsg);

 class_read_double("omega0l_prop",pba->int_parameters[1]);
 class_read_double("omega0m_prop",pba->int_parameters[2]);
 class_read_int("int_parameters_size",pba->int_parameters_size);

                              }
```

We added the feature of choosing in the `.ini` file the pre-programmed interacting models by defining a readable string called `"interacting_function"`.

```
class_call(parser_read_string(pfc,"interacting_function",&string3,&flag5,
    errmsg),
                 errmsg,errmsg);
if (flag5 == _TRUE_){
        if ((strstr(string3,"constant") != NULL) ||
         (strstr(string3,"CONSTANT") != NULL)) {
          pba->interacting_function = constant;}

        else if ((strstr(string3,"wang") != NULL) ||
         (strstr(string1,"WANG") != NULL)) {
          pba->interacting_function = wang;}

        else if ((strstr(string3,"martinelli") != NULL) ||
         (strstr(string1,"MARTINELLI") != NULL)) {
          pba->interacting_function = martinelli;}

        else if ((strstr(string3,"parab") != NULL) ||
         (strstr(string1,"PARAB") != NULL)) {
          pba->interacting_function = parab;}

        else {
          class_stop(errmsg,"incomprehensible input '%s' for the field
```

```
22              'interacting function'",string3);}
23                      }
```

3.3.2 Modifying Background Module

The principal aim of modifying this module is to implement the background equations of the Interacting Model. As we mentioned above, we followed the structure of a cosmology with a scalar field. The first step is to define a flag, that when is active indicates the presence of our interacting fluid. For the scalar field the flag was "scf", in our case we used "int" which stands for the interacting fluid. When this flag is active the definition of the functions of our model is made.

```
1 if (pba->has_int == _TRUE_)
2   {
3     rho_l_int = pvecback_B[pba->index_bi_rho_l_int]; //value of
    interacting Dark Energy density, indicating it is a {B} parameter.
4     rho_c_int = pvecback_B[pba->index_bi_rho_c_int]; //value of
    interacting Dark Matter density, indicating it is a {B} parameter.
5     H_aux=sqrt(rho_tot-pba->K/a/a);//value of Hubble parameter H, K is the
     spatial curvature.
6     pvecback[pba->index_bg_Q_int]=Q_int(pba,rho_l_int,rho_c_int,a,H_aux);
    //value of interacting parameter Q defined as {A} parameter.
7     rho_tot += pvecback[pba->index_bg_rho_l_int]+pvecback[pba->
    index_bg_rho_c_int]; //Adds our densities to the total density.
8     p_tot += -pvecback[pba->index_bg_rho_l_int];//Adds the contribution of
     interacting Dark Energy to total pressure.
```

Next we added the background equations (2.72), (2.73), where the notation `d[y]` stands for a derivative with respect to conformal time.

```
1  if (pba->has_int == _TRUE_){
2     dy[pba->index_bi_rho_c_int]=-y[pba->index_bi_a]*pvecback[pba->
    index_bg_Q_int]-3.*y[pba->index_bi_rho_c_int]*y[pba->index_bi_a]*
    pvecback[pba->index_bg_H];
3     dy[pba->index_bi_rho_l_int]=y[pba->index_bi_a]*pvecback[pba->
    index_bg_Q_int];
4                               }
```

In order to integrate, the initial conditions are needed: for Martinelli's interacting function the analytical solutions (2.79),(2.80) were implemented; for Wang's interacting function, the analytical solutions (2.82), (2.83) were also implemented assuming $\alpha_a = 0$, but we found that replacing $\alpha_0 \to \alpha_0 + \alpha_a$ the initial conditions worked better for the

general case in which $\alpha_a \neq 0$. If there were no analytical solutions available, we used those for ΛCDM. Recall that these initial conditions only work as a starting point for the shooting method already discussed.

```
if(pba->has_int == _TRUE_){
    switch (pba->interacting_function) {
      case constant:
      int_Q0 = pba->int_parameters[0];
      omega0l_prop = pba->int_parameters[1];
      omega0m_prop = pba->int_parameters[2];
      pvecback_integration[pba->index_bi_rho_l_int]=
      omega0l_prop*pba->H0*pba->H0;
      pvecback_integration[pba->index_bi_rho_c_int]=
      (omega0m_prop)*pba->H0*pba->H0*pow(pba->a_today/a,3);
      break;
      case wang:
      alpha_0 = pba->int_parameters[0];
      omega0l_prop = pba->int_parameters[1];
      omega0m_prop = pba->int_parameters[2];
      alpha_a = pba->int_parameters[3];
      A=omega0l_prop*pba->H0*pba->H0*pow(omega0l_prop*pba->H0*
      pba->H0+omega0m_prop*pba->H0*pba->H0,alpha_0+alpha_a);
      B=omega0m_prop*pba->H0*pba->H0*pow(omega0l_prop*pba->H0*
      pba->H0+omega0m_prop*pba->H0*pba->H0,alpha_0+alpha_a);
      pvecback_integration[pba->index_bi_rho_l_int]=
      A*pow((A+B*(pow(a,-3*(1+alpha_0+alpha_a)))),-(alpha_0+alpha_a)/
      (1+alpha_0+alpha_a));
      pvecback_integration[pba->index_bi_rho_c_int]=
      pow((A+B*(pow(a,-3*(1+alpha_0+alpha_a)))),1/(1+alpha_0+alpha_a))-
      A*pow((A+B*(pow(a,-3*(1+alpha_0+alpha_a)))),-(alpha_0+alpha_a)/
      (1+alpha_0+alpha_a));
      break;
      case martinelli:
      q0 = pba->int_parameters[0];
      omega0l_prop = pba->int_parameters[1];
      omega0m_prop = pba->int_parameters[2];
      pvecback_integration[pba->index_bi_rho_l_int]=
      omega0l_prop*pba->H0*pba->H0*pow(a,-q0);
      pvecback_integration[pba->index_bi_rho_c_int]=
      omega0m_prop*pba->H0*pba->H0*pow(a,-3)+
      omega0l_prop*pba->H0*pba->H0*(q0/(q0-3))*(pow(a,-3)-pow(a,-q0));
      break;
                                          }

```

Implementing new interacting Q models is now easy, we only have to define the parameters for each particular model and associate them to an input of `int_parameters`. We introduced here the Constant, Martinelli's and Wang's interacting functions via equations (2.77) and (2.81).

```
double Q_int(struct background *pba, double rho_l_int, double rho_c_int,
   double a, double H_aux)
  {
  switch (pba->interacting_function) {
      case constant:
               {
              double int_Q0 = pba->int_parameters[0];
              return int_Q0;
              break;
               }
      case martinelli:
               {
               double q0=pba->int_parameters[0];
               return -q0*H_aux*rho_l_int;
               break;
               }
      case wang:
               {
double alpha_0=pba->int_parameters[0], alpha_a=pba->int_parameters[3];
return 3*(alpha_0+alpha_a*(1-a))*H_aux*rho_l_int*rho_c_int/(rho_l_int+
   rho_c_int);
               break;
               }

                                    }
  }


```

3.3.3 Modifying the Perturbations Module

First we have to introduce Eq.(2.98) and then we have to add the contribution of our model to the perturbations frame of CLASS.

```
if (pba->has_int == _TRUE_) {
  ppw->delta_rho_int = ppw->pvecback[pba->index_bg_rho_c_int]*y[ppw->pv->
   index_pt_delta_int];
  ppw->delta_rho += ppw->delta_rho_int;
  ppw->rho_plus_p_tot += ppw->pvecback[pba->index_bg_rho_int];
```

```
5                                   }
```

Next we introduced the perturbation equation Eq.(2.100) for the interacting model. It is important to remember that this equation is only valid in the synchronous gauge and for the Dark Matter Geodesic Model. [1]

```
1 if (pba->has_int == _TRUE_) {
2         dy[pv->index_pt_delta_int] =
3           -metric_continuity+a*y[pv->index_pt_delta_int]*pvecback[pba->
    index_bg_Q_int]/pvecback[pba->index_bg_rho_c_int];
4                                   }
```

In order to evolve the perturbations, initial conditions are needed. We used those from Eq.(2.104).

```
1 if (pba->has_int == _TRUE_) {
2           ppw->pv->y[ppw->pv->index_pt_delta_int] =
3           3./4.*ppw->pv->y[ppw->pv->index_pt_delta_g];
4                                   }
```

3.4 Running CLASS

Running CLASS is simple, we only have to define all the needed cosmological parameters in the `.ini` file, open a terminal on the PC, go to the directory where CLASS is stored and give the following instruction in the terminal

```
1 ./class archivename.ini
```

Immediately the terminal will display information about the realization of the different stages of the code, some cosmological information and, if succeeded, the route and name where the output data will be stored. We present here and example of this display for one particular execution of CLASS

```
1 Reading input parameters
2 Computing unknown input parameters
3 Stage 1: background
4 omega_int shooting -0.000592495
5 omega0m_target shooting -0.00113418
6  -> found 'omega0l_prop = 2.430682e-02'
7  -> found 'omega0m_prop = 4.635692e-01'
```

[1] Note that `metric_continuity` stands for $\frac{h'}{2}$ with h the trace of perturbations matrix defined in Eq.(2.99).

```
Shooting completed using 9 function evaluations
 -> matched budget equations by adjusting Omega_int = 9.516329e-01
Running CLASS version v2.9.0
Computing background
 -> age = 12.268000 Gyr
 -> conformal age = 11778.827269 Mpc
 -> pba->Neff = 3.046000
    Details of interacting model:
     -> Omega_int = 0.951633, wished 0.951633
     -> parameters: [Q0] =
                    [0.000, 0.024, 0.464]
 -> radiation/matter equality at z = 5582.473812
    corresponding to conformal time = 68.768535 Mpc
 ------------------------------ Budget equation ----------------------
 ---> Nonrelativistic Species
-> Bayrons                      Omega = 0.0482754        , omega =
    0.022032
-> Cold Dark Matter             Omega = 1e-10            , omega =
    4.56381e-11
 ---> Relativistic Species
-> Photons                      Omega = 5.41867e-05      , omega =
    2.47298e-05
-> Ultra-relativistic relics    Omega = 3.74847e-05      , omega =
    1.71073e-05
 ---> Other Content
-> Interacting Model            Omega = 0.951633         , omega =
    0.434307
 ---> Total budgets
 Radiation                      Omega = 9.16714e-05      , omega =
    4.18371e-05
 Non-relativistic               Omega = 0.0482754        , omega =
    0.022032
 Other Content (Interacting Model)                    Omega = 0.951633
       , omega = 0.434307
 TOTAL                          Omega = 1                , omega =
    0.456381
 ---------------------------------------------------------------------
 Computing thermodynamics with Y_He=0.2453
 -> recombination at z = 1094.732512 (max of visibility function)
    corresponding to conformal time = 243.875895 Mpc
    with comoving sound horizon = 126.261515 Mpc
    angular diameter distance = 10.527160 Mpc
    and sound horizon angle 100*theta_s = 1.094599
    Thomson optical depth crosses one at z_* = 1090.750887
    giving an angle 100*theta_* = 1.097121
```

```
 -> baryon drag stops at z = 1064.885804
    corresponding to conformal time = 248.645600 Mpc
    with comoving sound horizon rs = 128.426224 Mpc
 -> reionization with optical depth = 0.073403
    corresponding to conformal time = 3366.950072 Mpc
Computing sources
Computing primordial spectra (analytic spectrum)
Computing linear Fourier spectra.
 -> sigma8=1.19135 for total matter (computed till k = 1.00203 h/Mpc)
No non-linear spectra requested. Nonlinear calculations skipped.
Computing transfers
Computing unlensed harmonic spectra
Computing lensed spectra (fast mode)
Writing output files in output/pruebacambmpk00_...
```

The archives that are stored containing all the output data are under this configuration:

- `background.dat` Contains the data related to background quantities like $\{\rho_c, \rho_\Lambda, \rho_b, H, d_{lum}, d_{ang}, Q...\}$.
- `cl.dat` Contains the CMB power spectrum C_ℓ.
- `cllensed.dat` Contains the lensed CMB power spectrum.
- `pk.dat` Contains the matter power spectrum $P(k)$.
- `parameters.ini` A complete list of cosmological parameters introduced in the `.ini` archive.
- `unusedparameters.dat` The unused cosmological parameters.

3.4.1 Commentary about Standard Cosmology parameter Basis

It is important to remark that from the ΛCDM parameter basis $\{A_s,\ n_s,\ \Omega_\Lambda,\ \Omega_m,\ \Omega_b,\ \tau_{reio}\}$ we kept fixed all the six parameters. In Table(3.1) we present a summary of this fixed values extracted from the `.ini` file. This values were fixed for all interacting models.

Parameter	A_s	n_s	Ω_b	Ω_Λ	Ω_m	τ_{reio}
Value	2.215×10^{-9}	0.9619	0.04827	0.6889	0.260666759	0.073403

Table 3.1: ΛCDM fixed parameter basis

3.5 Plotting the Numerical Output and Regions of Validity for the Interacting Model Parameters

When we obtained the final version of the modified CLASS, we immediately noticed that for some values of the interacting parameters we obtained negative values for some densities. We then found a specific range for the parameters of each interacting model where the interaction between Dark Matter and Dark Energy keeps positive the corresponding energy densities ρ_c and ρ_Λ. If we put values outside these regions, the output of CLASS gives warnings when finding a negative value for some energy density and then the program stops abruptly. Some authors noticed this behavior [35, 36]. They argue that interacting models like the one presented in this work break the weak energy condition and we verified that this in fact occurs for extreme values of the interacting parameters. This is understandable since we propose an energy exchange between Dark Energy and Dark Matter so we can not put arbitrary values for the parameters of the model or the energy densities could become negative. For this reason and in order to avoid this issue we found the following regions of validity reported in Table(3.2), for the interacting parameters where the weak energy condition holds through all evolution of the Universe. Finally we plotted the numerical output data varying each interacting parameter inside its region of validity.

Interacting function	Parameter with region of validity
Constant	$-4 \times 10^{102}\ \text{Mpc}^{-5} \leq \text{Q}_0 \leq 4 \times 10^{102}\ \text{Mpc}^{-5}$
Martinelli	$-21 \leq q_0 \leq 0.8$
Wang	$-0.99 \leq \alpha_0,\ \alpha_a \leq 6.3$

Table 3.2: Interacting model parameters and their region of validity.

4

Results

We present in this chapter plots of the numerical output of CLASS with the implemented Dark Energy-Dark Matter model. For details of the modifications of the CLASS code and a complete list of cosmological parameters, please see the Methodology chapter.

4.1 Comparison with Analytic Results

It is extremely important to check that the numerical integration performed by the modified CLASS code is correct. In order to verify this important topic we found in the literature the analytical solutions for Martinelli's and Wang's interacting models Eqs.(2.79) and (2.82) respectively. These analytical solutions can be found for a reduced model of the Universe where are only exist the interacting Dark Energy and Dark Matter. In that case with the Friedmann equation closes the differential equation system and we can be solve analytically. Despite the simplicity of the constant interacting function we did not find an analytical solution for the reduced model. Note that CLASS considers a more realistic scenario where also are considered ultra-relativistic species and baryons. Therefore a comparison between the reduced analytical solution and the CLASS output is not formally exact.

In Figs. (4.1) to (4.4) we present the comparison of the analytical and numerical densities ρ_c and ρ_Λ with the corresponding percentage difference between them, finding that despite the already commented limitations the analytical solution agrees well with the numerical output of CLASS with a maximal percentage difference of 0.35%. We

considered that this result is enough to conclude that the numerical integrations carried out by the CLASS code are correct since the analytical and numerical solutions are completely independent and have variations of less than 0.35%. This is important because we can now implement new models for the interacting function Q, even if they do not have a reduced analytical solution and we would know that numerical integration will be correct.

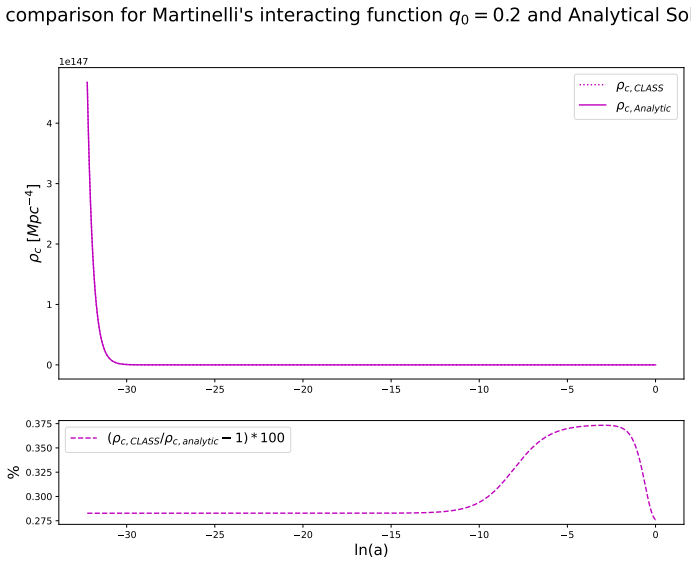

Figure 4.1: ρ_c comparison - Between numerical CLASS output and analytical model defined in Eqs.(2.79) and (2.80).

4.2 Ω's for the Interacting Models

In this section we plot the Ω density parameters for radiation Ω_r, interacting Dark Energy Ω_Λ and matter Ω_m. Where Ω_m contains the contribution of baryons Ω_b and interacting Dark Matter Ω_c versus the expansion factor a.

In Fig.(4.5) we present the density parameters Ω for the case of a constant interacting function $Q = Q_0$. Recall from the background equation in the constant interacting model Eq.(2.72) that $Q_0 > 0$ directly implies $\rho'_\Lambda > 0$ and therefore we will have a subsequent positive contribution to Ω'_Λ. We can see this effect in Fig.(4.5), at the epoch when Dark Energy increases, the Ω_Λ lines with $Q_0 > 0$ have a greater slope than the

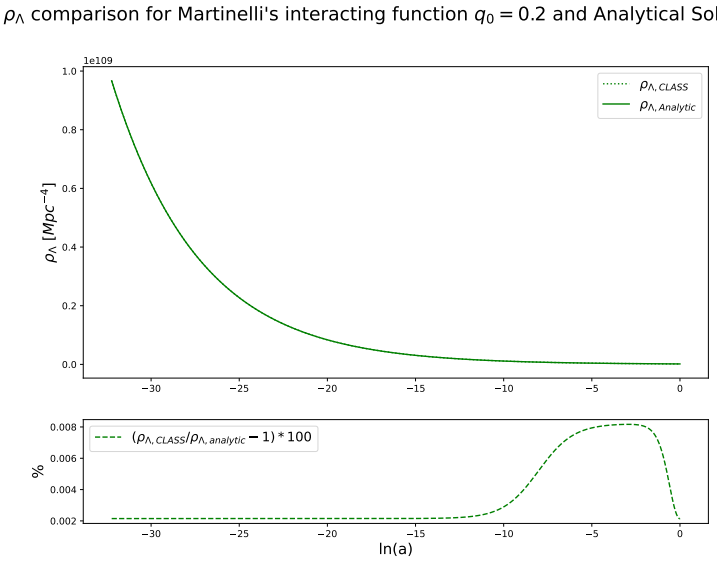

Figure 4.2: ρ_Λ comparison - Between numerical CLASS output and analytical model defined in Eqs.(2.79) and (2.80).

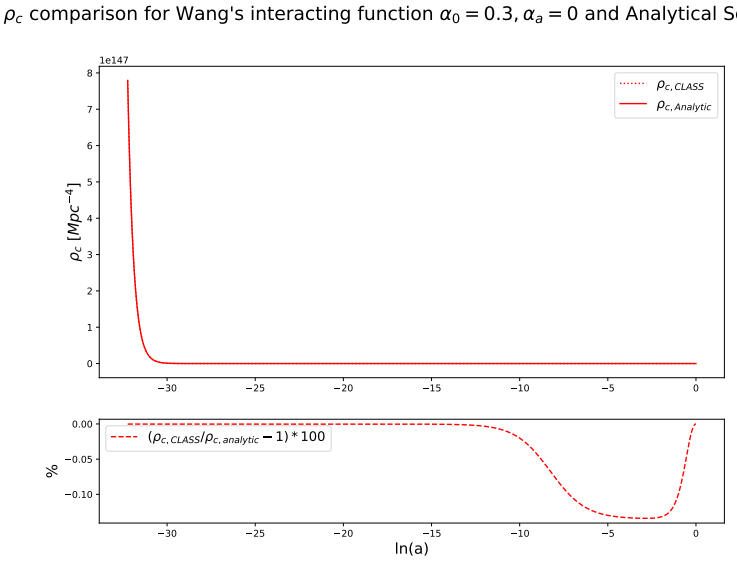

Figure 4.3: ρ_c comparison - Between numerical CLASS output and analytical model defined in Eqs.(2.82) and (2.83).

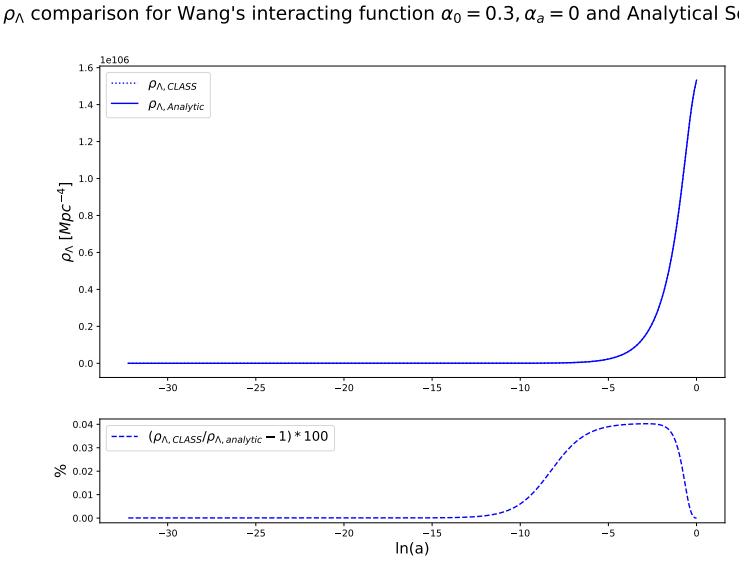

Figure 4.4: ρ_Λ comparison - Between numerical CLASS output and analytical model defined in Eqs.(2.82) and (2.83).

ΛCDM reference. In fact they tend to be vertical. The reason behind this feature is that we kept fixed the parameter Ω_Λ^0, which has to be reached with greater slope, causing that the Ω_Λ lines with $Q_0 > 0$ are below the ΛCDM reference line. This means that despite the ρ'_Λ increasing there is less content of Dark Energy respect to ΛCDM for $ln(a) < 0$. We can also see in Fig.(4.5) that this lack of Dark Energy is reflected in an increment of Ω_m respect to ΛCDM model, since the Ω_m lines for $Q_0 > 0$ are above the respective ΛCDM line for all $ln(a) < 0$. This enhanced Dark Matter causes radiation-matter equality to happen earlier and a later matter-Dark Energy time of equality respect to ΛCDM as we can see in Fig.(4.5). The case $Q_0 < 0$ can be thought in an analogous but opposite way.

In Fig.(4.6) for the Martinelli's interacting model $Q = -q_0 H \rho_\Lambda$ we noticed that Q and q_0 carry opposite sign, since the Hubble parameter H and the energy density ρ_Λ are positive definite. For this interacting model, the minus in the definition makes in a similar analysis to the Constant interacting case $q_0 > 0$ favors an increase of Dark Energy in the Universe. This causes a later matter-radiation equality and an earlier matter-Dark Energy equality respect to ΛCDM model. For $q_0 < 0$ we can observe in Fig.(4.6) the inverse situation, matter-radiation equality happens earlier and matter-

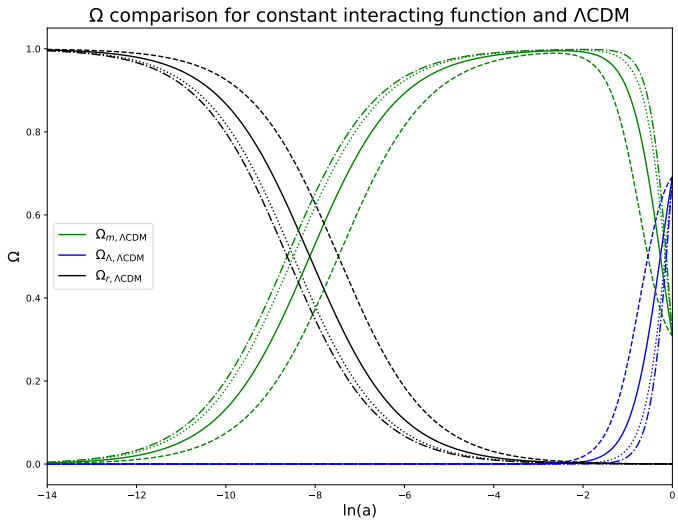

Figure 4.5: Ω 's for Constant Interacting Model - Solid line for ΛCDM, (- - -) for $Q_0 = -2.7 \times 10^{102}\text{Mpc}^{-5}$, (·····) for $Q_0 = 2.7 \times 10^{102}\text{Mpc}^{-5}$ and (-·-·-) for $Q_0 = 4 \times 10^{102}\text{Mpc}^{-5}$, with Q_0 defined in Eq.(2.76).

Dark Energy happens later than in the ΛCDM model. In Figs.(4.7), (4.8) we plot the corresponding Ω's for Wang's interacting model

$$Q = 3(\alpha_0 + \alpha_a(1-a))H\frac{\rho_c\rho_\Lambda}{\rho_c + \rho_\Lambda},$$

keeping fixed one of the two parameters to see their individual effect. From the above definition we see that both parameters α_0 and α_a have the same sign as Q. So we verify in each figure that occurs the same case as in the constant interacting function already discussed. Positive parameters α_0 and α_a cause a matter-radiation equality to happen earlier and a matter-Dark Energy equality to happen later than in the ΛCDM model. Negative values of the parameters have the contary effect.

In general we notice a change in time of density parameter equalities, this will become important in the following discussions especially when analyzing the Power Spectra for the different interacting models.

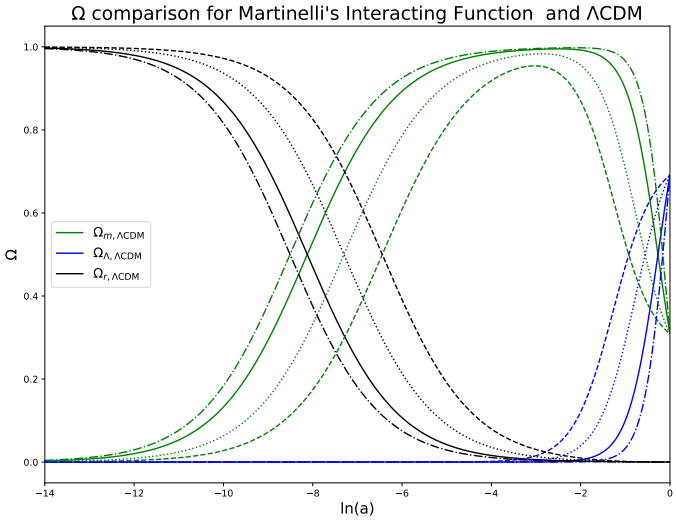

Figure 4.6: Ω 's for Martinelli's Interacting Model - Solid line for ΛCDM, (- - -) for $q_0 = 0.8$, (·····) for $q_0 = 0.6$ and (-·-·-) for $q_0 = -0.8$, with q_0 defined in Eq.(2.77).

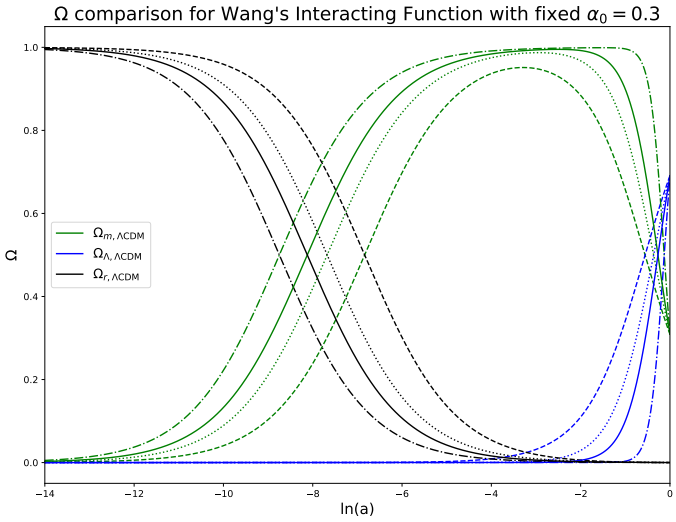

Figure 4.7: Ω 's for Wang's Interacting Model - Solid line for ΛCDM, and in this figure $\alpha_0 = 0.3$ is fixed, while (- - -) stands for $\alpha_a = -0.9$, (·····) for $\alpha_a = -0.6$ and (-·-·-) for $\alpha_a = 0.9$, with α_0 and α_a defined in Eq.(2.81).

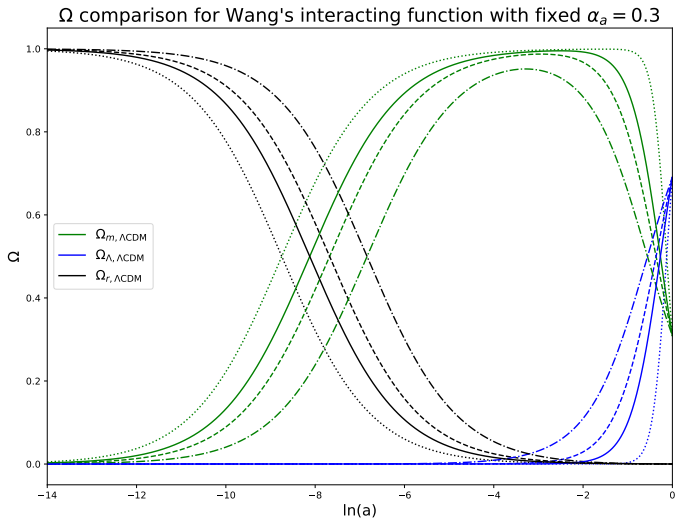

Figure 4.8: Ω 's for Wang's Interacting Model - Solid line for ΛCDM, and in this figure $\alpha_a = 0.3$ is fixed, while (- - -) stands for $\alpha_0 = -0.6$, (·····) for $\alpha_0 = 0.9$ and (-·-·-) for $\alpha_0 = -0.9$, with α_0 and α_a defined in Eq.(2.81).

4.3 Hubble Parameter for the Interacting Models

In Fig.(4.9) we show CLASS's output corresponding to the Hubble parameter H vs. redshift z, in the interval $z \in [0, 5]$ since it is a reasonable observable interval. We see that the interacting model affects notably the Hubble parameter. We see that lines for interacting parameters that augment ρ'_Λ present an increase in the value of the Hubble parameter , meanwhile lines with a decrease in value of the Hubble parameter are those which enhance ρ'_m. We plotted for Constant and Martinelli's interacting functions parameters with different sign, then we observed in Fig.(4.9) that the cases $Q_0 > 0$ and $q_0 < 0$ increase the Hubble parameter respect to the ΛCDM reference line and the opposite cases are below this reference line. The situation for Wang's model having two parameters is a bit different, we chose plotting a pair of parameters with different sign. The particular choice of the plotted parameters for Wang's model resulted in a smaller Hubble parameter for each $z > 0$ with respect to ΛCDM model.

In general we notice that the cases $Q_0, \alpha_0, \alpha_a < 0$ and $q_0 > 0$ for the different interacting models tend to flattened the obtained curve in Fig.(4.9). All this cases contribute to an increment of ρ'_m and as already discussed a consequent enhancement

of Dark Energy. This essentially means that this enhancement of Dark Energy tends to the de Sitter Universe [37] where the Hubble parameter is constant.

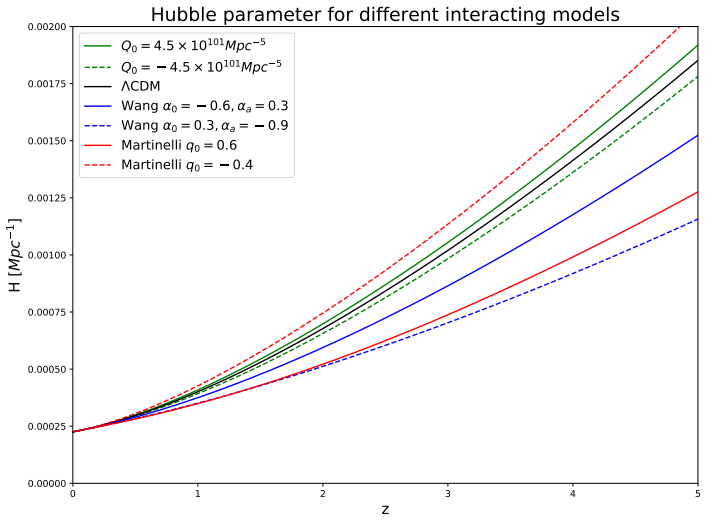

Figure 4.9: Hubble parameter - H for different interacting models with H defined in Eq.(2.29).

4.4 CMB Power Spectrum for the Interacting Models

In this section we present the CLASS output relative to the CMB power spectrum for the different interacting models, in each figure we vary the parameters of the corresponding model in order to see their effects on the CMB power spectrum.[1]

In Fig.(4.10) we observe the CMB power spectrum for constant interacting function, for different values of the parameter Q_0. We proceed now to analyze the resulting CMB power spectrum related to the above effects for constant interacting function.

- Global Amplitude. We note that global amplitude does not change since the amplitude of the primordial spectrum A_s is kept fixed.

[1]Please, note that we have plotted $\ell(\ell+1)C_\ell/2\pi$ versus ℓ. Also notice that the horizontal axis of figures has two different scales, for $\ell < 100$ the scale is logarithmic and for $\ell > 0$ the scale is lineal. The reason of plotting this way is that for the first ℓ's we can observe the Sachs-Wolfe plateau which we have discussed in theory of the CMB power spectrum.

- Global tilt. Global tilt has no changes in the interacting model.
- First peak scale. We note that the first peak scale changes by only a tiny value.
- Amplitude of first peaks. We notice that the amplitude of the first peaks change depending on the value of Q_0. We think this has a simple physical explanation: we note in Fig.(4.10) that power spectra with $Q_0 < 0$ have a greater amplitude of their first peaks with respect to ΛCDM reference spectrum. This effect is due the fact that for $Q_0 < 0$ radiation-matter equality takes place later, expanding in time the radiation domination era during which the gravitational enhancements are higher respect to those in a matter dominated Universe. The case $Q_0 > 0$ can be explained in an analogous and opposite situation where the radiation-matter equality happens earlier.
- Ratio of odd to even peaks. We see that the ratio of odd-even peaks changes for the constant interacting function. For $Q_0 < 0$ the amplitude of the second peak is bigger than the third and for $Q_0 > 0$ occurs the contrary situation. Since we know $Q_0 > 0$ favors the quantity of Dark Matter this means that if Dark Matter is enhanced the amplitude of the second peak reduces.
- Damping envelope. This envelope is considered to cover the peaks approximately from the third one. We see from Fig.(4.10) that the amplitude from the third peak and above do not change considerably, they are only displaced in the horizontal ℓ scale. We know from the theory that this envelope depends strongly on the diffusion length of photons at decoupling and the interacting model does not affect this quantity.
- Sachs-Wolfe plateau tilting. We notice for $\ell < 100$ with aid of the horizontal logarithmic scale that the Sachs-Wolfe plateau slope changes depending on the value of Q_0. We can see in Fig.(4.10) that the tilting of the plateau increases for $Q_0 < 0$, we have discussed this phenomena in the theory chapter concluding that the duration of Dark Energy domination makes greater the tilting, and indeed this is the case for $Q_0 < 0$. We already discussed that matter-Dark Energy equality happens earlier, making the Dark Energy domination epoch longer. Contrary, the case $Q_0 > 0$ causes a reduced Dark Energy domination era and therefore the plateau tilting is less pronounced.

- Amplitude for $\ell > 40$. We do not expect a change in this feature of the CMB power spectrum since we kept fixed all parameters related to the optical reionization depth.

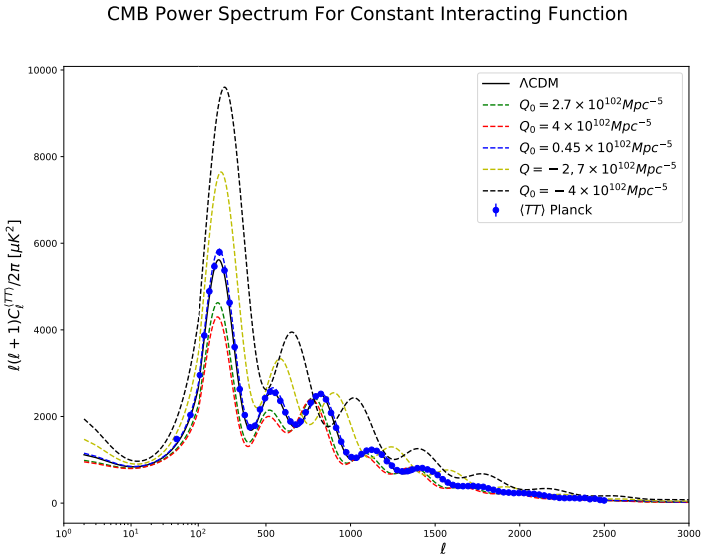

Figure 4.10: CMB Power Spectrum for Constant Interacting Model - Comparison between different values of Q_0, ΛCDM and Plack 2018 data, with Q_0 defined in Eq.(2.76).

In Fig.(4.11) we see the corresponding CMB power spectrum for the Martinelli's interacting function. We only find a trivial difference from the case of the constant interacting model. From the definition of the Martinelli's interacting function it carries an extra minus sign. This causes that now the peaks for $q_0 > 0$ are enhanced in amplitude. So the cases $Q_0 < 0$ for constant interacting function and $q_0 > 0$ for Martinelli's model are essentially equivalent.

In Figs.(4.12) and (4.13) we present the CMB power spectrum obtained for the Wang's interacting model keeping one of the parameters α_0 or α_a fixed respectively. We note that the effects produced in these figures are analogue to the constant interacting function, the cases $Q_0 < 0$ and $\alpha_0 < 0$ or $\alpha_a < 0$ produce similar effects and can be explained in a similar way already discussed.

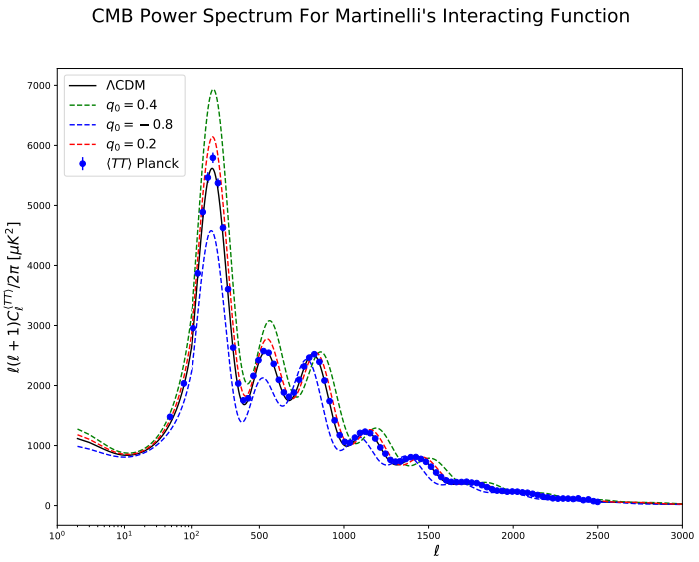

Figure 4.11: CMB Power Spectrum for Martinelli's Interacting Model - Comparison between different values of q_0, ΛCDM and Plack 2018 data, with q_0 defined in Eq.(2.77).

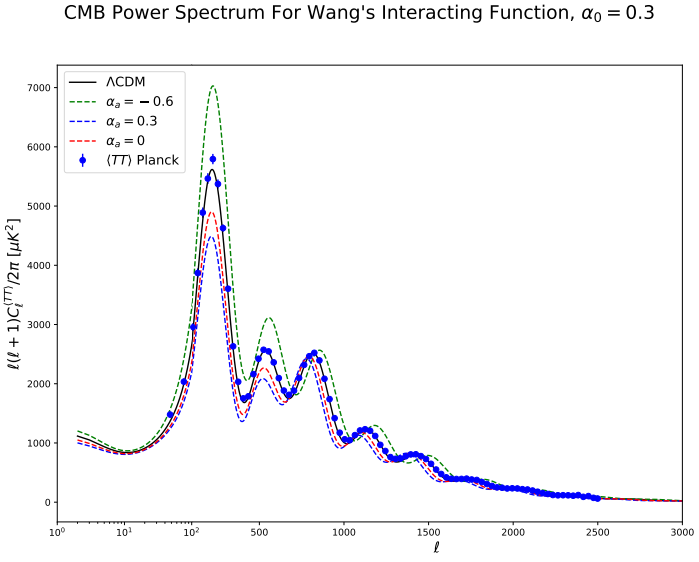

Figure 4.12: CMB Power Spectrum for Wang's Interacting Model - Comparison between different values of α_a (α_0 is kept at 0.3), ΛCDM and Planck 2018 data, with α_0 and α_a defined in Eq.(2.81).

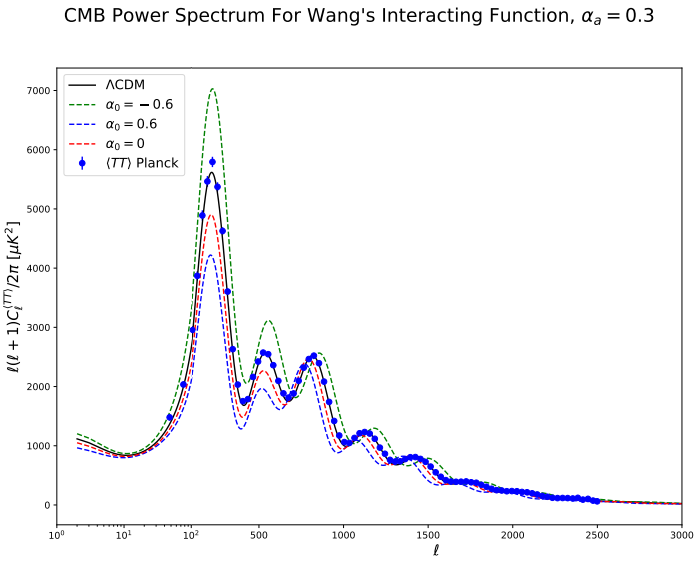

Figure 4.13: CMB Power Spectrum for Wang's Interacting Model - Comparison between different values of α_0 (α_a is kept at 0.3), ΛCDM and Planck 2018 data, with α_0 and α_a defined in Eq.(2.81).

4.5 The Matter Power Spectrum for the Interacting Models

In this section we present the CLASS's output corresponding to the Matter Power Spectrum for the different interacting models.

In Fig.(4.14) we can see that the global maxima of the spectrum at $k = k_{eq}$ moves horizontally in the k axis depending on the value of the parameter Q_0. We observe that for $Q_0 < 0$ this maxima move towards smaller values of k and as Q_0 gets positive this moves to greater values of k with respect to the ΛCDM model. We remember that $Q_0 < 0$ implies a later radiation-matter time of equality, so we find that if a_{eq} increases then k_{eq} in the matter power spectrum reduces its value. Also for $k > k_{eq}$ the oscillations' amplitude increase as Q_0 becomes more negative, we see a similar effect in the CMB power spectrum where for negative Q_0 the amplitude of the anisotropies increase. This is clear for us, we know from the theory that perturbations for all the components of the Universe are strongly coupled in some regimes.

In Fig.(4.15) we see the corresponding Matter Power spectrum for Martinelli's in-

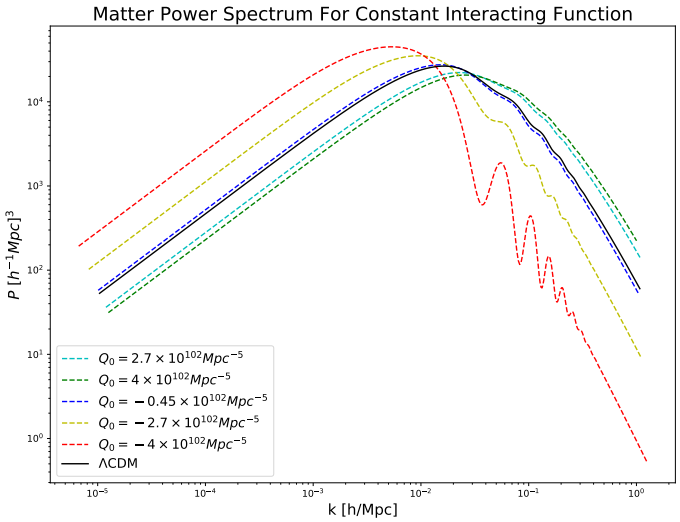

Figure 4.14: Matter Power Spectrum for Constant Interacting Model - Comparison between different values of Q_0 and ΛCDM, with Q_0 defined in Eq.(2.76).

teracting model, again the cases $Q_0 < 0$ in the constant interacting model and $q_0 > 0$ are practically equivalent.

In Figs.(4.16) and (4.17) we present the Matter Power Spectrum for Wang's interacting model. We see similar effects to the case of the Constant interacting function when we kept fixed one parameter of Wang's model and allow the other to vary. Respectively the more negative α_0 or $\alpha_a < 0$ the more oscillations we find for $k > k_{eq}$ and also k_{eq} reduces its value.

4.6 Effective Equation of State for the Interacting Models

In Fig.(4.18) we present the effective equation of state for the interacting Dark Energy, we recall here that it is not a formal equation of state but it is an indicator of the dynamics of Dark Energy since it is proportional to ρ'_Λ. We defined in Eq.(2.87) this effective equation of state $w_{eff} \equiv -1 - \frac{Q}{3H\rho_\Lambda}$, finding it proportional to the interacting function Q and inversely proportional to the factor $H\rho_\Lambda$. This is important because we can define interacting models having the form $Q = 3H\rho_\Lambda\chi$, with $\chi = \chi(a, \rho_c, \rho_\Lambda, ...)$ in order to do keep the same degrees of freedom to the model. In this case, the effective

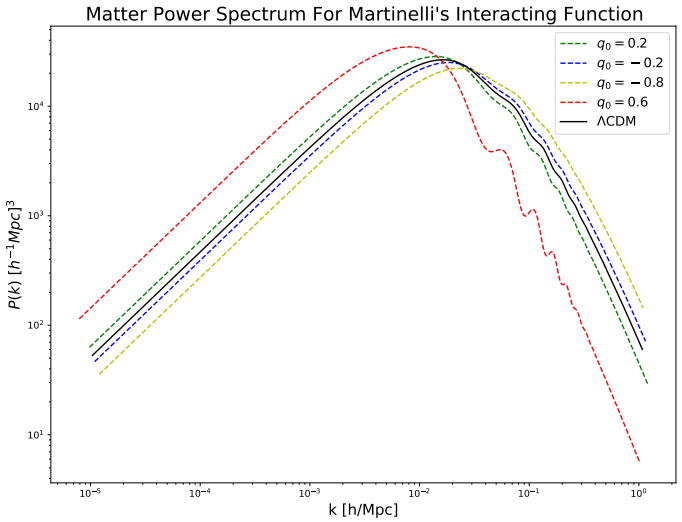

Figure 4.15: Matter Power Spectrum for Martinelli's Interacting Model - Comparison between different values of q_0 and ΛCDM, with q_0 defined in Eq.(2.77).

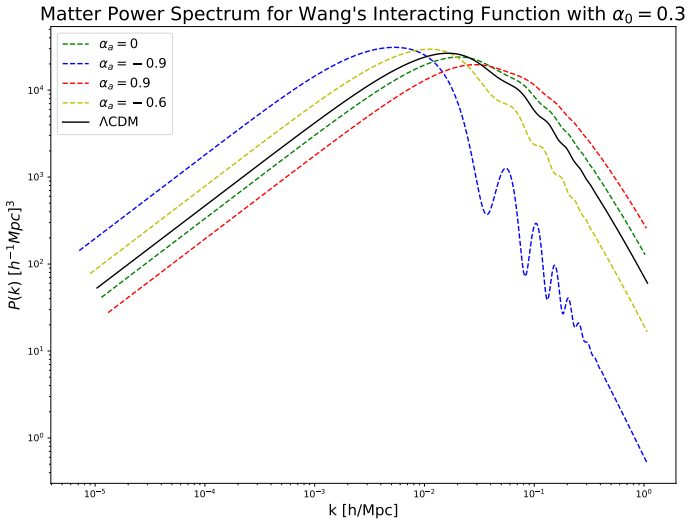

Figure 4.16: Matter Power Spectrum for Wang's Interacting Model - Comparison between different values of α_a (α_0 is kept at 0.3) and ΛCDM, with α_0 and α_a defined in Eq.(2.81).

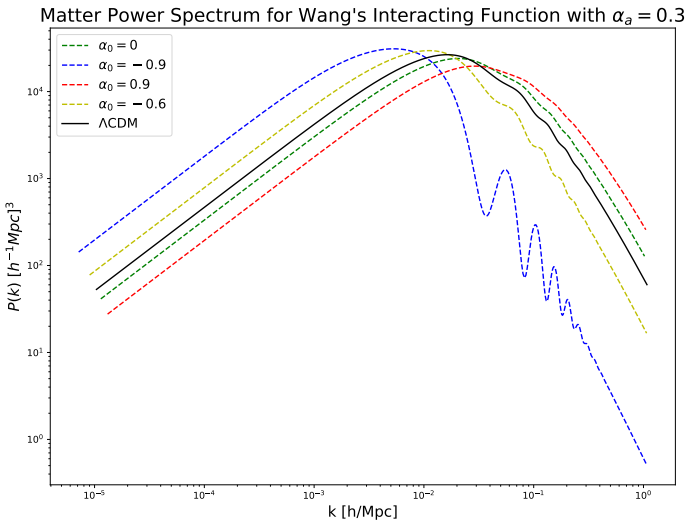

Figure 4.17: Matter Power Spectrum for Wang's Interacting Model - Comparison between different values of α_0 (α_a is kept at 0.3) and ΛCDM, with α_0 and α_a defined in Eq.(2.81).

equation of state reduces to $w_{eff} = -1 - \chi$ and we have a huge freedom to model the form of this effective equation of state. Some authors [38] have found effective equations of state but do not have a theoretical model, hence the interacting model could be an interesting proposal in order to explain these results.

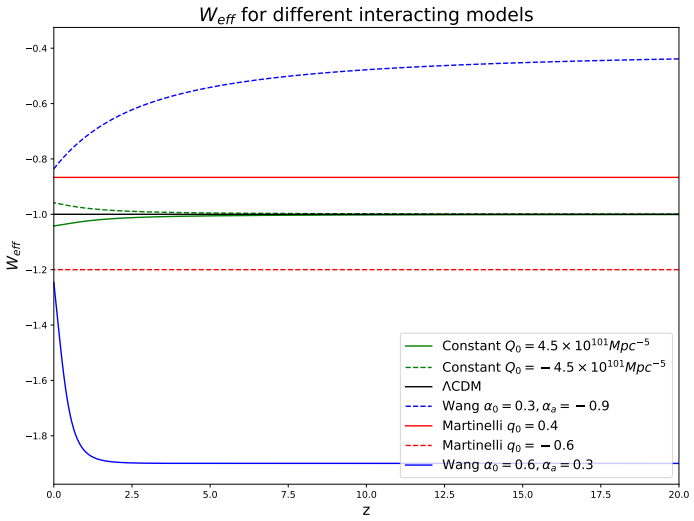

Figure 4.18: Effective equation of state for interacting Dark Energy - Comparison between different W_{eff} defined in Eq.(2.87).

5

Conclusions

In this work we build the conceptual and computational tools to study models with interaction between Dark Matter and Dark Energy. Some of these models might reduce the tensions in the measurements of the Hubble constant in a future work. The implementation of new interacting models is now easy and we have reported how to do it in some simple steps. So in a practical amount of time we can obtain wide numerical cosmological information at background and at first level in perturbations theory. We checked that the numerical integration were carried correctly by comparing with analytic solutions, finding a maximal percentage difference of 0.35%. This numerical information can be now subjected to experimental tests and have been compared with the corresponding ΛCDM results finding notable differences that make suitable the model to a posterior parameter fitting. Each studied interacting model had specific parameters for which we have found regions of validity where they satisfy the weak condition of energy. We obtained the evolution of the density parameters Ω by finding that in the interacting scenario, the time of equality for matter-radiation and the posterior matter-Dark Energy in fact changed depending on the sign and value of the interacting function Q. We found that the case $Q > 0$ increased ρ'_Λ and contra-intuitively enhanced ρ_c in order to reach the fixed parameters Ω_{Lambda} and Ω_c at present time. This increment of ρ_c caused an earlier matter-radiation equality and a later matter-Dark Energy time of equality. So the particular model parameters that favored a positive Q presented this behavior. The case $Q < 0$ was found to be directly the opposite. These changes in equality times affected the posterior results.

We obtained the matter and CMB Power Spectrum for the different models. We

analyzed in the CMB power spectrum the following characteristics in the interacting model. The global amplitude and global tilt of the spectrum were not changed, since we kept fixed the parameters A_s and n_s that govern them and the interacting scenario did not induce any change. The scale of the first peak changed but only by a little amount of a few ℓ's. The amplitude of the first peaks changed and we found that they were enhanced for $Q < 0$, the reason is that the radiation-matter equality happens later for $Q < 0$ with respect to the ΛCDM one, this causes an extension in time of the radiation dominated era where the gravitational enhancement effects are more present than in a matter-dominated Universe. The ratio of odd-even peaks changed: we found that the Dark Matter density increases for $Q > 0$ and at the same time the amplitude of the second peak reduces. So the more Dark Matter present in the Universe, the more reduced the second peak becomes. The damping envelope of all CMB power spectrum were not changed in the interacting models, nor the amplitude for large ℓ where possible reionization effects could be present. The Sachs-Wolfe plateau tilting for $\ell < 100$ notably changes in the interacting scenario, for $Q < 0$ the tilting increases, meaning that an extension in time of Dark Energy domination favored the tilting of the plateau. In regard to the matter Power Spectrum we observed that the maximum of the spectrum at $k = k_{eq}$ gets displaced horizontally in the k axis depending on the value and sign of the interacting function Q. The more negative Q, the smaller k_{eq}, so we concluded that if a_{eq} the value of the expansion factor at the time of radiation-matter augment then the corresponding k_{eq} reduces. For the case $Q > 0$ the contrary effect takes place. Another observed effect was that for $k > k_{eq}$ the more negative Q, the more oscillations found in the matter power spectrum and more amplitude in the corresponding CMB power spectrum.

Some proposals have been made in this area of study, in principle we analyze here the models proposed by Wang [10] and Martinelli [11]. Wang's model was proposed to explain the discrepancy found in the measurement of the 21-cm brightness temperature performed by the EDGES team [39], respect to the value predicted by ΛCDM model. There they found a non-trivial constrain on the parameters of the Wang's model, that fitted the experimental results. We found that the values of these fitted parameters are inside our region of validity for Wang's model. On the other hand, for the Martinelli's model they conclude that the no-interaction scenario is compatible at a 95% confidence level in all their parameter estimations. So, the pursuit of a good interaction model

that agrees well with all possible observational data remains open. In this line, our work represents a good opportunity in the area of the interacting scenario, because our basic idea is to give the bases and tools to propose and test new models, i.e., we are not restricted to one particular model.

This work opens the possibility to study models that reproduce a w_{eff} as the one found in [38]. The model proposed here can be designed to cross the phantom divide for $w_{eff} = -1$, we already know that an interacting function of the type $Q = 3\rho_\Lambda H\chi$ will lead us to an effective equation of state for the Dark Energy $w_{eff} = -1 - \chi$, then we have the freedom of choosing χ in a particular and desired way. We also still need to explore the different models using MontePython [12] and therefore to constrain the parameters of a given interacting model. This task generally requires less work than modifying CLASS code, the principal difference is that the former requires more computational power than the later. Therefore we still have a wide panorama to explore in this dark interacting sector.

One of the limitations of this work is that we did not include a microscopic explanation for the energy exchange, since we are interested in directly compare it with observations and then in a posterior analysis determine the viability of a deeper theoretical analysis. This work is based on a macroscopic energy exchange between the Dark Matter and Dark Energy, this allowed us to obtain the Power Spectra for the matter and for the CMB, but we did not begin from a Lagrangian formulation. Another limitation is that we can find in the literature interacting models that break the weak energy condition [35, 36]. We found that this indeed happens but for extreme values of the interacting parameters, to solve this issue we found regions of validity for the interacting parameters where the weak energy condition holds. These regions were easy to estimate, the CLASS code automatically stops if any non-positive value of some density is found. Another possible issue is that some particular interacting models, for example [40], once constrained with observational data trivial values of the parameters were preferred. But all this conclusions are subjected to one particular model, here we have the opportunity of exploring new ones.

We are in a good position to study interacting models given the tools created. The proposal in this thesis is to study one of the many variations of the ΛCDM model and we have explored this option by finding the corresponding matter and CMB Power Spectrum. And principally important we have the basis for new posterior explorations

in the dark interacting sector. We obtained a viable way to modify a standard model like the ΛCDM one, by adding new features to some cosmological components of the model. Following the rules of General Relativity we have now the possibility of obtaining data ready to be compared with the latest observations, we also gained insights in how this proposal affects essential characteristics of the Universe like times of equality between different components and how this information is contained in the Power Spectra that carry the fingerprints of the real Universe when measured. So we have tested in a theoretical way a possible version of the Universe, where the assumed components Dark Matter and Dark Energy interact, but of course only observations will dictate if this idea is viable or not.

Bibliography

[1] Andrew Liddle. *An introduction to modern cosmology.* John Wiley & Sons, 2015. ix, 5, 9, 13

[2] Suvodip Mukherjee, Archisman Ghosh, Matthew J. Graham, Christos Karathanasis, Mansi M. Kasliwal, Ignacio Magaña Hernandez, Samaya M. Nissanke, Alessandra Silvestri, and Benjamin D. Wandelt. **First measurement of the Hubble parameter from bright binary black hole GW190521**, 2020. 2

[3] D. W. Pesce, J. A. Braatz, M. J. Reid, A. G. Riess, D. Scolnic, J. J. Condon, F. Gao, C. Henkel, C. M. V. Impellizzeri, C. Y. Kuo, and et al. **The Megamaser Cosmology Project. XIII. Combined Hubble Constant Constraints**. *The Astrophysical Journal*, **891**(1):L1, Feb 2020.

[4] A J Shajib, S Birrer, T Treu, A Agnello, E J Buckley-Geer, J H H Chan, L Christensen, C Lemon, H Lin, M Millon, and et al. **STRIDES: a 3.9 per cent measurement of the Hubble constant from the strong lens system DES J0408-5354**. *Monthly Notices of the Royal Astronomical Society*, **494**(4):6072–6102, Mar 2020.

[5] Geoff C-F Chen, Christopher D Fassnacht, Sherry H Suyu, Cristian E Rusu, James H H Chan, Kenneth C Wong, Matthew W Auger, Stefan Hilbert, Vivien Bonvin, Simon Birrer, and et al. **A SHARP view of H0LiCOW: H0 from three time-delay gravitational lens systems with adaptive optics imaging**. *Monthly Notices of the Royal Astronomical Society*, **490**(2):1743–1773, Sep 2019.

[6] Koushik Dutta, Anirban Roy, Ruchika, Anjan A. Sen, and M. M. Sheikh-Jabbari. **Cosmology with low-redshift observations: No signal for new physics**. *Physical Review D*, **100**(10), Nov 2019.

[7] M. J. Reid, D. W. Pesce, and A. G. Riess. **An Improved Distance to NGC 4258 and Its Implications for the Hubble Constant**. *The Astrophysical Journal*, **886**(2):L27, Nov 2019.

[8] Wendy L. Freedman, Barry F. Madore, Dylan Hatt, Taylor J. Hoyt, In Sung Jang, Rachael L. Beaton, Christopher R. Burns, Myung Gyoon Lee, Andrew J. Monson, Jillian R. Neeley, and et al. **The Carnegie-Chicago Hubble Program. VIII. An Independent Determination of the Hubble Constant Based on the Tip of the Red Giant Branch**. *The Astrophysical Journal*, **882**(1):34, Aug 2019. 2

[9] Julien Lesgourgues. **The Cosmic Linear Anisotropy Solving System (CLASS) I: Overview**, 2011. 3, 39

[10] Yuting Wang and Gong-Bo Zhao. **Constraining the Dark Matter Vacuum Energy Interaction Using the EDGES 21 cm Absorption Signal**. *The Astrophysical Journal*, **869**(1):26, dec 2018. 3, 24, 70

[11] Matteo Martinelli, Natalie B Hogg, Simone Peirone, Marco Bruni, and David Wands. **Constraints on the interacting vacuum-geodesic CDM scenario**. *Monthly Notices of the Royal Astronomical Society*, **488**(3):3423–3438, 07 2019. 3, 24, 70

[12] Benjamin Audren, Julien Lesgourgues, Karim Benabed, and Simon Prunet. **Monte Python: Monte Carlo code for CLASS in Python**, July 2013. 3, 71

[13] William Huggins. **XXI. Further observations on the spectra of some the stars and nebulae, with an attempt to determine therefrom whether these bodies are moving towards or from the earth, also observations on the spectra of the sun and of comet II., 1868**. *Philosophical Transactions of the Royal Society of London*, (158):529–564, 1868. 5

[14] Edwin Hubble. **A relation between distance and radial velocity among extra-galactic nebulae**. *Proceedings of the national academy of sciences*, **15**(3):168–173, 1929. 6

[15] A. Friedmann. **Über die Krümmung des Raumes**. *Zeitschrift fur Physik*, **10**:377–386, January 1922. 7

BIBLIOGRAPHY

[16] G. Lemaitre. **Expansion of the universe, A homogeneous universe of constant mass and increasing radius accounting for the radial velocity of extra-galactic nebulae**. *Monthly Notices of the Royal Astronomical Society*, **91**:483–490, March 1931.

[17] H.P. Robertson. **Kinematics and World-Structure**. *The Astrophysical Journal*, **82**:284, November 1935.

[18] A.G. Walker. **On Milne's Theory of World-Structure**. *Proceedings of the London Mathematical Society*, **42**:90–127, January 1937. 7

[19] Roger Penrose. **Gravitational Collapse and Space-Time Singularities**. *Physical Review Letters*, **14**(3):57–59, January 1965. 12

[20] Alexei A Starobinsky. **Dynamics of phase transition in the new inflationary universe scenario and generation of perturbations**. *Physics Letters B*, **117**(3-4):175–178, 1982. 12

[21] Arno A Penzias and Robert Woodrow Wilson. **A measurement of excess antenna temperature at 4080 Mc/s.** *The Astrophysical Journal*, **142**:419–421, 1965. 14

[22] N. Aghanim, Y. Akrami, M. Ashdown, J. Aumont, C. Baccigalupi, M. Ballardini, A. J. Banday, R. B. Barreiro, N. Bartolo, and et al. **Planck 2018 results**. *Astronomy and Astrophysics*, **641**:A6, Sep 2020. 15

[23] James M Bardeen. **Gauge-invariant cosmological perturbations**. *Physical Review D*, **22**(8):1882, 1980. 15, 18

[24] Robert V. Wagoner. **Scalar-Tensor Theory and Gravitational Waves**. *Phys. Rev. D*, **1**:3209–3216, Jun 1970. 16

[25] EM Lifshitz. **Zh. Ehk sp. Teor. Fiz. 16, 587: J**. *Phys. USSR Acad. Sci*, **10**:116, 1946. 18

[26] Lev Davidovich Landau. *The classical theory of fields*, **2**. Elsevier, 2013. 18

[27] David Wands, Josue De-Santiago, and Yuting Wang. **Inhomogeneous vacuum energy**. *Class. Quant. Grav.*, **29**:145017, 2012. 20, 21

[28] Gabriela Caldera-Cabral, Roy Maartens, and L. Arturo Ureña López. **Dynamics of interacting dark energy**. *Phys. Rev. D*, **79**:063518, Mar 2009.

[29] Eleonora Di Valentino, Alessandro Melchiorri, and Olga Mena. **Can interacting dark energy solve the H_0 tension?** *Phys. Rev. D*, **96**:043503, Aug 2017. 21

[30] P. Astier, J. Guy, N. Regnault, R. Pain, E. Aubourg, D. Balam, S. Basa, R. G. Carlberg, S. Fabbro, D. Fouchez, I. M. Hook, D. A. Howell, H. Lafoux, J. D. Neill, N. Palanque-Delabrouille, K. Perrett, C. J. Pritchet, J. Rich, M. Sullivan, R. Taillet, G. Aldering, P. Antilogus, V. Arsenijevic, C. Balland, S. Baumont, J. Bronder, H. Courtois, R. S. Ellis, M. Filiol, A. C. Gonçalves, A. Goobar, D. Guide, D. Hardin, V. Lusset, C. Lidman, R. McMahon, M. Mouchet, A. Mourao, S. Perlmutter, P. Ripoche, C. Tao, and N. Walton. **The Supernova Legacy Survey: measurement of Ω_M, Ω_Λ and w from the first year data set**. *Astronomy and Astrophysics*, **447**(1):31–48, February 2006. 22

[31] Christian M. Müller. **Cosmological bounds on the equation of state of dark matter**. *Phys. Rev. D*, **71**:047302, Feb 2005. 22

[32] Yuting Wang, David Wands, Lixin Xu, Josue De-Santiago, and Alireza Hojjati. **Cosmological constraints on a decomposed Chaplygin gas**. *Physical Review D*, **87**(8):083503, 2013. 26

[33] Steven Weinberg et al. *Cosmology*. Oxford university press, 2008. 28, 33, 35

[34] Steven Weinberg. **Adiabatic modes in cosmology**. *Phys. Rev. D*, **67**:123504, Jun 2003. 29

[35] Jussi Valiviita, Elisabetta Majerotto, and Roy Maartens. **Large-scale instability in interacting dark energy and dark matter fluids**. *Journal of Cosmology and Astroparticle Physics*, **2008**(07):020, jul 2008. 52, 71

[36] S Carneiro, HA Borges, R von Marttens, JS Alcaniz, and W Zimdahl. **Unphysical properties in a class of interacting dark energy models**. *arXiv preprint arXiv:1909.10336*, 2019. 52, 71

[37] Willem De Sitter. **On the relativity of inertia. Remarks concerning Einstein's latest hypothesis**. *Proc. Kon. Ned. Acad. Wet*, **19**(2):1217–1225, 1917. 60

[38] Gong-Bo Zhao, Marco Raveri, Levon Pogosian, Yuting Wang, Robert G Crittenden, Will J Handley, Will J Percival, Florian Beutler, Jonathan Brinkmann, Chia-Hsun Chuang, et al. **Dynamical dark energy in light of the latest observations**. *Nature Astronomy*, **1**(9):627–632, 2017. 67, 71

[39] JD Bowman, AEE Rogers, RA Monsalve, TJ Mozdzen, and N Mahesh. **An absorption profile centred at 78 megahertz in the sky-averaged spectrum. 2018**. *Nature*, **555**:67. 70

[40] Micol Benetti, Welber Miranda, Humberto A Borges, Cassio Pigozzo, Saulo Carneiro, and Jailson S Alcaniz. **Looking for interactions in the cosmological dark sector**. *Journal of Cosmology and Astroparticle Physics*, **2019**(12):023, 2019. 71